CHAPTER 1
INTRODUCTION

CHAPTER 1
INTRODUCTION

1.1 Introduction

Industrial drives have become the standard for motion operation and control in the heavy, medium and small scale industries. These drives constitute motors, power converters and control algorithms for processing the electrical energy. Power converters and control algorithms needs power electronic components, microcontrollers and embedded systems to drive the motor at desired operating points and to achieve the energy efficient performance. However, the power electronic devices and microcontroller/embedded system generate harmonics and needs reactive power from the supply source. Further, these devices and controllers due to their inherent non-linearity draw a non sinusoidal current from the supply. In the present study, a three phase PWM converter fed induction motor drives using vector control and direct torque have been simulated for desired performance of the induction motor.

1.2 Industrial Drives

Industries widely use induction motor drives for various speed applications in a broad power preference from fraction of horse power to megawatts. The major reasons of the widespread use of these machines are their robustness and inexpensiveness, less maintenance and simple construction. Moreover, with comparison to the dc motor, induction motor can be used in hostile and unstable surroundings since there are no issues related to commutation spark and corrosion. Along with these mentioned advantages induction motor also provides sensor less control scheme for speed control. The attention in sensor less control scheme of induction motor drives has been developed extensively over the last few years because of their many plus points, such as mechanical robustness and simple construction of the control mechanism. The induction motor drives system with the development of the vector control technology makes them attractive for industries.

1.3 Control Schemes for Industrial Drives

The different control schemes implemented for induction motor drives are scalar control, vector or field orientation control and direct torque control.

1.3.1 Scalar control

Scalar control as the name suggests, considers the variation in magnitude of the control variable only, and does not take notice of the coupling effect in machine. The flux of the machine can be controlled by the variation in voltage, and the torque can be by variation in frequency or slip of the motor. This implies, flux is a function of voltage and torque is a function of frequency. Although, scalar control is simple to execute but it gives rather substandard performance. Due to the intrinsic coupling phenomenon of scalar control of drives, the system becomes sluggish and unstable. Moreover, their importance has diminished recently because of the superior performance of vector control drives.

1.3.2 Field Oriented Control

The principle of vector control or field oriented control was introduced by Blaschke in 1972 [1]. Vector control technique is used to realize induction motor drives with dc motor characteristics. The vector control basically applies the decoupled control of flux and torque in the motor. In DC machine the field flux is perpendicular to the armature flux and do not interact with each other. Therefore, by adjusting the field current the DC machine flux can be controlled and independent to this the torque can be controlled by varying the armature current [2]. But the control of an AC machine is not as simple because of the interactions between the stator and the rotor fields owing to their non orthogonal orientations to each other and varying orientations as per the operating conditions. AC machine can attain DC machine like performance characteristics by keeping a fixed perpendicular orientation of the field and armature fields. This can be achieved by orienting the stator current with respect to the rotor flux in a manner such that independent control is attained. In the present work the application of flux oriented vector control on induction motors has been discussed.

1.3.3 Direct Torque Control (DTC) of Induction Motor

The direct torque control of inverter fed induction machine was introduced by M. Depenbrock in 1988 [3]. In DTC scheme the stator resistance value is the only

machine parameter used to estimate the stator flux, therefore it is least dependent on the machine model. The least dependency to machine parameters of DTC scheme makes it simpler than field-oriented control. The main attributes of DTC scheme are direct controlling of torque and flux, indirect controlling of stator voltages and currents and gives approximately sinusoidal stator currents and stator fluxes. These attributes leads to advantages such as co-ordinate axis transforms is absent in the control scheme. The controllers such as voltage modulation block and PID controller for motor torque and flux are also not needed in the control algorithm. The DTC control mechanism has the advantage of rapid torque response time, much better than the field oriented control or vector control.

1.4 Three Phase PWM Converter

The converters may be broadly classified as uncontrolled and controlled [4]. The uncontrolled converters use diodes as the semiconductor power switch. On the other hand controllable power semiconductors switches like metal oxide semiconductor field effect transistors (MOSFETS), bipolar junction transistors (BJT), insulated gate bipolar transistors (IGBT) and thyristors are used for controlled converters [5]

In industrial applications where three phase ac voltages are available, controlled three phase rectifiers are used, because of their fewer ripples in the current waveform and a high power handling capability. The three phase PWM converter designed for 415V, 50Hz industrial load supply offers solution to reduce the harmonic distortion caused by non linear industrial drives. The three main parts to design a PWM converter are phase locked loop block (PLL), current controller and a pulse width modulation (PWM) generator. The PLL block automatically amends the phase of input signal with the generated signal using feedback loop system. The voltages calculated from PLL are used for three phase abc to dq transform and send to decoupled current and voltage controllers. The reference voltages generated by controller are sent to the PWM block to create the switching pattern. The complete schematic diagram of the system is shown in figure 1.1.

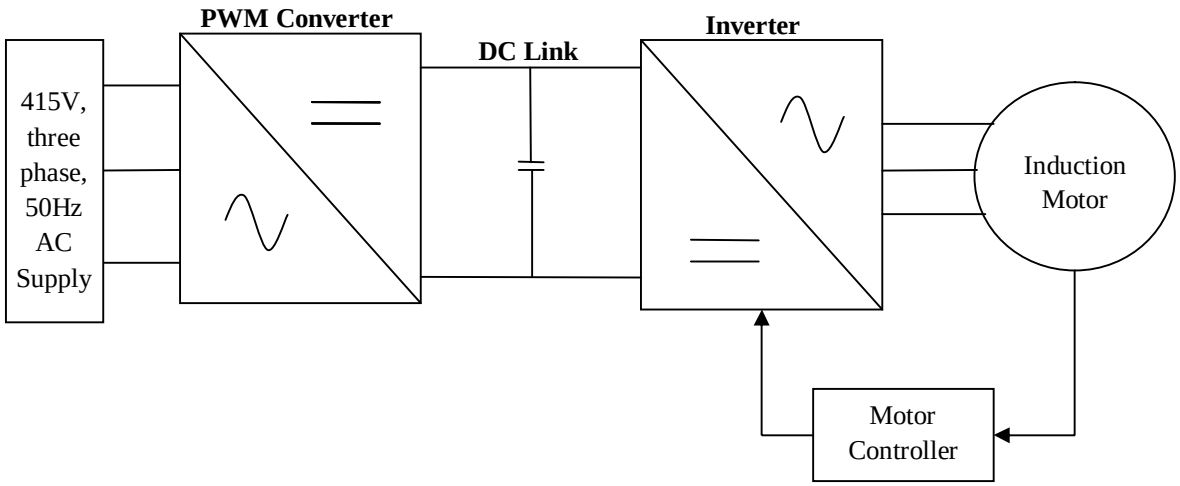

Figure 1.1. Complete schematic diagram of the proposed system

1.5 Objective of Thesis

The industries make use of variable speed induction motor drives for various plant processes in the assembly line. These induction motor drives comprises of an induction motor, a speed controller and an inverter. The objective of this dissertation is to design and compare the performance of the vector controlled and direct torque controlled induction motor. Furthermore, due to the non linear nature of the drives system, they are responsible for harmonic distortion and poor power factor. So, the work is taken to the next level by designing an efficient PWM converter which is capable of effectively controlling the harmonics and maintaining the power factor to unity.

1.6 Preview of The Thesis

The whole work of dissertation is organized in 8 chapters. Chapter1 presents the general introduction of the industrial drives, PWM converter, drives control strategies and objective of thesis. Chapter 2 contains the literature review of the thesis for supply side unity power factor control and indirect vector control of induction motor. Chapter 3 elaborates the model of induction motor drives and control algorithms which include direct torque control and field oriented control. Chapter 4 discusses the design consideration of ac to dc three phase PWM converter. Chapter 5 describes the simulink model for unity power factor supply to vector controlled induction motor drives. Different control blocks are explained in this

chapter. Chapter 6 contains the simulink results. The results are presented and analysed in this chapter. Chapter 7 contains the conclusions based on the simulink results. It also includes the further scope of work done so far.

1.7 Conclusion

A brief introduction of industrial drives, control scheme for industrial drives and PWM converter is presented in this chapter. The objective of thesis is explained with the organization of thesis.

CHAPTER 2
LITERATURE REVIEW

CHAPTER 2
LITERATURE REVIEW

2.1 Introduction

This chapter contains a brief review of previous work on topics dealt within this thesis without trying to be exhaustive in anyway. The dissertation review deals with the studies of industrial drives and associated related work being carried out on different types of control schemes of induction motor drives during last few decades. The study were conducted to understand the non linear characteristics of induction motor drives and to search an efficient and effective method to reduce harmonics and maintain the power factor to unity. The references cited in this chapter are also representative rather than exhaustive.

2.2 Field Oriented Control Of Industrial Motor Drives

The widely implemented technique for industrial drives control is vector control. This technique decouple the flux and torque commands, hence make the AC motor drives characteristics analogous to the separately excited DC motor drives without compromising on the quality of the dynamic performance of the drives.

There are two ways of vector control techniques to apply to induction motor drives

(a) Direct or feed- back control

(b) Indirect or feed forward control

In direct Field orientation control the angle is obtained by the terminal voltages & currents, while as in indirect Field orientation control, the angle is obtained by using rotor position measurement & machine parameter estimation.

Blaschke in 1972 gave the concept of vector control technique [1] and the other, mechanisms known as the indirect or feed forward method was invented by Hasse (1969) [6], [7] which were interpreted into practical implementation later by Gabriel et al (1980), Leonhard (1985) and many others with the progress in microprocessors and microcomputers along with power electronics.

Field oriented control has come out as a dominant means for controlling inverter fed induction motors. The complex functions required by field oriented

control may be executed by microprocessors on line, thus greatly reducing the necessary control hardware [8], [9].

The essential condition to get fine control performance is to make the induction motor parameters of field-oriented control overlap with the real parameter of the motor. It was Takayoshi [10] who described a new identification technique utilizing injected negative sequence components. It is shown that the stator as well as rotor resistance and leakage inductance can be determined live while the motor is driving the load. The theory is verified with a complete hybrid computer simulation of a PWM inverter fed induction motor drives with field oriented control.

The performance of induction motor drives is mainly determined by the gating Pulses feeding the inverter. A current control technique using hysteresis [11], [12] can be applied for determining the pulse pattern. With this method, fast response current loop will be obtained and knowledge of load parameter is not required. However this method can cause variable switching frequency of inverter and produce undesirable harmonic generation.

Bimal K Bose and others proposed the fuzzy logic based on-line efficiency optimization control for indirect vector control of induction motor [13]. The extended fuzzy logic based efficiency optimization to flux oriented vector controlled induction motor is explained which shows the advantage of fast convergence with inherent adaptive step size signals of fuzzy control [14].

The high performance of the control of speed, toque is established through vector control of induction motor drives. The vector control method gives same characteristics to the inverter fed induction motor drive as of separately excited dc motor [15]. The vector control gives decoupled control of the rotor flux magnitude and the torque-producing current, with a fast, near-step change in torque achievable. The rapid torque response is attained by rotor flux estimation of the induction motor. For the indirect vector control method, the estimation of the rotor flux position is dependent on the value of rotor resistance. Also parameter calculation algorithms, like the extended Kalman filter, can be used for the evaluation of rotor resistance. The vector-controlled induction motor drive evaluation system can be executed in two techniques. The first method uses a real machine and the second approach is the simulation of system with suitable vector controller and a current-regulated pulse width modulation (PWM) inverter.

The first method has the advantages of inherently including elements such as the actual noise present, the PWM waveform and nonlinear device, and sensor characteristics that are hard or impracticable to include in a simulation [16]. Alternatively, simulation of system has the advantage of observing all magnitudes readily, altering parameters to investigate their effect and assisting to debug estimation and control routines. Sensor noise can also be added to simulate the characteristics of actual sensors in addition to testing the ability of parameter identification techniques to manage with noisy measurements. Tests on higher power and speed rated motor can be easily performed by just changing the parameters.

Induction motor drives are appropriate for various speed applications as they are robust, gives rigid torque speed characteristics and have high performance control algorithm. The flux is estimated by the rotor speed. However rotor speed measurement is always hard, not practical and many times unfeasible. These reasons demand the need of estimating the rotor speed by means of only the stator voltage and current measurements. This estimator could be useful, not only for speed feedback as part of speed control loop in servo drives, but also for diagnosis of the drives when speed measurement is available. Since all the necessary electrical variables are available within the power electronics controller, speed estimates and measurements could be compared. Note that estimation algorithms require calculation of the variable of interest, plus some averaging method to filter noise.

2.3 Direct Torque Control Induction Motor Drives

Direct torque control of induction motor was introduced by Depenbrock [3] in Germany and Takahashi [17] in Japan. It is used widely in industries because of its simple structure and rapid response of flux and torque. It is a technique broadly implemented for inverter-fed induction motor drives. The stator flux linkage and the electromagnetic torque are controlled directly in direct torque control technique for induction motor drives. This is possible because of the selection of an optimum inverter switching state from switching table. The selection of the switching state is made to limit the flux and the torque errors within their respective hysteresis bands and to attain the fastest torque response and highest efficiency at every instant. Direct torque control method is trouble-free than field-oriented method and is less

dependent on the motor parameters, as the stator resistance value is the only machine factor used to estimate the stator flux.

Study in this control scheme has been done in much method by many researchers. Shauder C studied to compare the criteria between DTC and Field Oriented Control. He compared the basic control strategies, dynamic performance and parameter sensitivity [18].

Buja, Casadei and Serra described the three of DTC based techniques implementing switching tables, space vector modulation and direct self control [19]. They used observation from an experiment to make a selection of the magnitude of the hysteresis band of the torque and flux to solve the problem of their tutorial. They also made comparison between DTC and FOC.

L Tang et al, gave a new control technique for reducing torque and flux ripple for induction motors using space vector modulation [20]. The basic idea of direct torque control is slip control, which is based on particular logical relationship between slip and torque is described. They also made comparison between DTC and FOC with conventional method.

A space vector pulse width modulation based direct torque control technique for three phase induction motor with theory of imaginary switching times was proposed by A. Kumar and H.R Keyhani [21, 22]. He eliminated the lengthy process of using reference voltage vector by determining effective time using imaginary time vector. Hence there he introduced significance decline in implementation time due to removal of look-up table.

C.Martins, gave the switching frequency imposition and ripple reduction techniques [23]. The strategy used multilevel converter in DTC drives to reduce torque ripples. They also studied performance of DTC using PI stator resistance comparator. This method estimated stator resistance.

Basic configuration of DTC includes of hysteresis controller, torque and flux estimator and switching table [24]. The instantaneous values of torque and flux are estimated from stator variables by using a closed loop estimator. Stator flux and torque may be controlled directly or indirectly by correctly choosing the inverter switching configurations.

Inputs of a three level hysteresis comparator are from the error between the estimated torque and the reference torque [25]. The error between the estimated flux

magnitude and reference stator flux magnitude is sent to input of two level hysteresis comparator.

With the switching table, the inverter voltage space vector is selected for each sampling period in order to keep the torque and stator flux magnitudes within the limits of two hysteresis bands.

2.4 PWM Converter for Industrial Drives

Pulse width modulation technique using sine triangle intersection was first proposed by Schönung and Stemmler in 1964 [26]. Due to the ease of implementation, the sinusoidal PWM is found in a wide range of applications. The application of PWM converter has become more predominant. J.W. Dixan and Boon T. Ooi proposed the topology and principle of the operation of current controlled PWM converter in the year 1987 [27]. S.B Dewan with R.Wu also gave the modeling of ac to dc PWM converter with fixed switching frequency during same time [28].
V.Blasko and V. Kaura proposed the mathematical modeling of three phase ac to dc voltage source converter [5]. This mathematical model of the power circuit of a three-phase voltage source converter (VSC) was developed in the stationary and synchronous reference frames. The mathematical model was then used to analyze and synthesize the voltage and current control loops for the VSC. Analytical expressions were derived for calculating the gains and time constants of the current and voltage regulators.

Bo Yin and Oruganti described the single input single output model for a three phase PWM converter [29]. He made the model segregating the d-axis and the q-axis dynamics through appropriate nonlinear feedforward decoupling while maintaining unity power factor operation. With the proposed model, the non minimum phase feature natural in an ac-to-dc converter becomes a simple righthalf-plane zero appearing in the small-signal control-to-output transfer function. This makes it possible to expand the system examination and control design techniques of dc–dc converters to the three-phase PWM converter The demonstration through closed-loop operation of the converter with both voltage mode and inner-current-loop-based schemes proved the effectiveness of the model.

Henghchun Mao et al gave the reduced order small signal model of a three phase PWM converter and also mentioned its applications in control system analysis

[30]. Hiti S, Boroyevich D., Cuadros, C proposed small signal modeling and control of three phase PWM converters in 1994 for industrial applications [31]. The design of current controller for 3 phase pwm converter with unbalanced input voltage was proposed by H.S Kim et al [32].

The carrier based PWM-VSI overmodulation analysis and design was explained with models by A.M Hava in 1988 [33]. He investigated the overmodulation region voltage gain characteristics and waveform quality of carrier-based pulse width - modulated (PWM) methods. A comparative evaluation of the modulator characteristics reveals the advantageous high-modulation range characteristics of discontinuous PWM methods and, in particular, the superior overmodulation performance of a discontinuous PWM technique. The results of the study were useful in designing, performance predestining, and developing of high-performance overmodulation approaches for PWM-VSI drives.

L.N Amuda presented a comprehensive explanation of a three-phase PLL (phase-locked loop) construction that fits the needs of utility connected PV systems [34]. The tuning of the PLL structure was also discussed as well as its performance under utility distorted conditions were tudied. Additionally, he introduced a new single-phase PLL topology. Its dynamic behaviour was evaluated and its quasi-instantaneous ability to detect phase, frequency and amplitude of the utility voltage was highlighted. Salamah A.M. also proposed the three phase lock loop for distorted utilities [35].

2.5 Conclusion

A survey of various power circuit configurations and control strategies has been carried out and presented in this chapter. Vector control of induction motor plays an important role in designing an industrial drives. The review of two control schemes of vector control named: field oriented control and direct torque control has been performed. The industrial drives is connected to an AC-to-DC converter which is a specially designed to mitigate current harmonics and gives unity power factor performance of the motor.

CHAPTER 3
MDELLING OF INDUSTRIAL DRIVES

CHAPTER 3
INDUSTRIAL DRIVES CONTROL SCHEME

3.1 Introduction

In India the power supply for domestic purpose and small power load is single phase, 240V, 50 Hz and for large loads is three phase, 415V, 50 Hz. The induction motor is the most popular motor used in consumer and industrial applications. The concept of this "sparkless" motor was first conceived by Nicola Tesla in the late nineteenth century. The motor does not have a brush/commutator structure like a DC motor has, which eliminates all the problems associated with sparking; such as electrical noise, brush wear, high friction, and poor reliability. The absence of magnets in the rotor and stator structures further enhances reliability, and also makes it very economical to manufacture. In high horsepower applications, the AC induction motor is one of the most efficient motors in existence.

The major reason why these machines are so robust and inexpensive is that no external current is required inside the rotor to create the revolving magnetic field. An induction machine consists fundamentally of two parts: the stator (the stationary part) and the rotor (the moving part). For a three-phase induction machine, three-phase sinusoidal voltages are applied to the windings of the stator. This creates a magnetic field. Because the voltages differ in phase by 120^0 with respect to each other, a revolving magnetic field is created that rotates in synchronism with the changing dominant poles around the cylindrical stator.

3.2 Salient Features of Induction Motor

Induction motor drives perform best when they are driven with sinusoidal voltages and currents. One of the advantages of induction motor drives is the incredibly smooth operation they can provide as a result of low torque ripple.

3.2.1 Working Principle of Three Phase Induction Motor

To achieve this, most induction motor drives consists of a slotted stator structure where the windings are placed in the slots with a sinusoidal winding distribution, resulting in a sinusoidal flux distribution in the airgap. This flux also links the rotor circuit, which consists of copper or aluminium bars shorted at each

end, and mounted on a stacked laminate structure comprised of soft iron, or other ferrous material. In most cases, motor efficiency can be increased by decreasing the rotor bar resistance. As the flux cuts across these conductors, a dØ/dt voltage is impressed across the rotor bars, which results in current flow in the rotor. In other words, current is induced in the rotor circuit from the stator circuit; much the same way that secondary current is induced from the primary coil in a standard transformer. This rotor current produces its own flux, which interacts with the stator mmf to produce torque. However, in order to achieve this dØ/dt effect on the rotor bars, the rotor cannot rotate at the same speed as the rotating stator field. As a result, induction motors are classified as asynchronous motors. The difference in rotational speed between the stator flux vector and the rotor is called slip. As more torque is required from the motor shaft, the slip frequency increases. In conclusion, the motor speed is a function of the number of stator poles, the motor torque (and consequently motor slip), and the frequency of the AC input voltage. The three phase topology represents an ideal choice for variable-speed applications.

3.2.2 Dynamic Model Of Induction Motor

A dynamic model of the machine subjected to control must be known in order to understand and design vector controlled drives. Due to the fact that every good control has to face any possible change of the plant, it could be said that the dynamic model of the machine could be just a good approximation of the real plant. Nevertheless, the model should incorporate all the important dynamic effects occurring during both steady-state and transient operations. Furthermore, it should be valid for any changes in the inverter's supply such as voltages or currents [2]. Such a model can be obtained by means of either the space vector phasor theory or two-axis theory of electrical machines. The three phase squirrel cage induction motor in synchronous rotating reference frame can be represented by the figure 3.1.

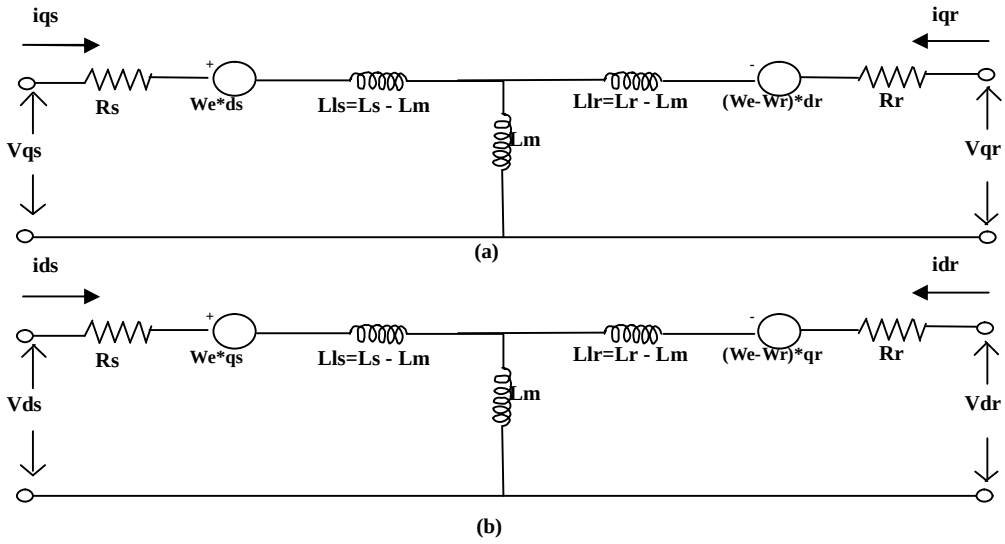

Figure 3.1 Equivalent circuit of an induction motor in the synchronous rotating reference frame, a) q-axis circuit b) d-axis circuit

The various parameters are calculated as under:

Voltage equations are

$$V_{qs} = R_s * i_{qs} + \frac{d\varphi_{qs}}{dt} + \omega_e \varphi_{ds} \quad (3.1)$$

$$V_{ds} = R_s * i_{ds} + \frac{d\varphi_{ds}}{dt} - \omega_e \varphi_{qs} \quad (3.2)$$

$$V_{qr} = R_r * i_{qr} + \frac{d\varphi_{qr}}{dt} + (\omega_e - \omega_r)\varphi_{dr} \quad (3.3)$$

$$V_{dr} = R_r * i_{dr} + \frac{d\varphi_{dr}}{dt} - (\omega_e - \omega_r)\varphi_{qr} \quad (3.4)$$

Flux equations are

$$\varphi_{qs} = L_{ls} * i_{qs} + (i_{qs} + i_{qr})L_m \quad (3.5)$$

$$\varphi_{qr} = L_{lr} * i_{qr} + (i_{qs} + i_{qr})L_m \quad (3.6)$$

$$\varphi_{ds} = L_{ls} * i_{ds} + (i_{ds} + i_{dr})L_m \quad (3.7)$$

$$\varphi_{dr} = L_{lr} * i_{dr} + (i_{ds} + i_{dr})L_m \quad (3.8)$$

Where V_{qs} & V_{ds} are the applied voltages to the stator; i_{ds}, i_{qs}, i_{dr}, & i_{qr} are the corresponding d & q axis currents; $\varphi_{qs}, \varphi_{qr}, \varphi_{ds}$ & φ_{dr} are the rotor & stator flux component; R_s, R_r are the stator & rotor resistances; L_{ls} & L_{lr} denotes the stator & rotor inductances, whereas L_m is the mutual inductance.

The electromagnetic torque equation is

$$T_e = \frac{3*P*L_m}{2*2*L_r} * (\varphi_{dr} i_{qs} - \varphi_{qr} i_{ds}) \quad (3.9)$$

Where *P* denotes the pole number of the motor

In case of vector control the *q*-component of the rotor field φ_{qr} would be zero. Then the electromagnetic torque is controlled only by *q*-axis stator current & becomes

$$T_e = \frac{3*P*L_m}{2*2*L_r} * (\varphi_{dr} i_{qs}) \quad (3.10)$$

3.3 Speed Control Scheme of Three Phase Induction Motor Drives

The different control schemes of induction motor drivess are including Scalar control, vector or field orientation control, direct torque and flux control, and adaptive control etc. But induction motor control drives are broadly classified in two category i.e. scalar control and vector control.

3.3.1 Scalar Control of Induction Motor

Scalar control as the name indicates, is due to magnitude variation of the control variable only, and disregards the coupling effect in machine. For example, the voltage of machine can be controlled to control the flux, and frequency or slip can be controlled to control the torque. However flux and torque are also function of voltage and frequency respectively. A scalar controlled drives gives somewhat inferior performance. Scalar control is easy to implement. Scalar controlled drives have been widely used in industry, but the inherent coupling effect (both torque and flux are function of voltage or current and frequency) gives sluggish response and system is easily prone to instability because of higher order (fifth order) system effect. To make it clearer, if torque is increased by incrementing the slip (the frequency), the flux tends to decrease .it has been noted that the flux variation is also sluggish. Decreases in flux then compensated by the sluggish flux control loop feeding an additional voltage. This temporary dipping of flux reduces the torque sensitivity with slip and lengthens the response time. However, their importance has diminished recently because of the superior performance of vector.

3.3.2Vector Field-oriented Control of Induction Motor Drives

FOC involves controlling the components of the motor stator currents, represented by a vector, in a rotating reference frame (with a d-q coordinate system)

[10]. In a special reference frame, the expression for the electromagnetic torque of the smooth-air-gap machine is similar to the expression of torque in a separately excited DC machine. In the case of induction machines, the control is normally performed in a reference frame aligned to the rotor flux space vector. To perform the alignment on a reference frame revolving with the rotor flux requires information about the modulus and the space angle (position) of the rotor flux space vector. The FOC algorithm is summarized as:

1. Measure the stator phase currents ia, ib and ic. If only the values of ia and ib are measured ic can be calculated as for balanced current ia + ib + ic = 0.

2. Transform the set of these three-phase currents onto a two-axis system. This conversion provides the variables iα and iβ from the measured ia , ib and ic values where id and iq are time-varying quadrature current values, as viewed from the stator's perspective. This conversion is popularly known as Clarke Transformation.

3. Calculate the rotor flux and its orientation.

4. Rotate the two-axis coordinate system such that it is in alignment with the rotor flux, using the transformation angle calculated at the last iteration of the control loop. This conversion provides the id and iq variables from iα and iβ. This step is more commonly known as the Park Transformation.

5. Flux error signal is formed using flux reference and estimated flux value. A PI controller is then used to calculate i*d using this error signal. i*q is generated using the reference torque value and the estimated flux value.

6. i*d and i*q are converted to a set of three phase currents to produce i*a, i*b, i*c.

7. i* a, i*b, i*c and ia, ib, ic are compared using hysterysis comparator to generate.

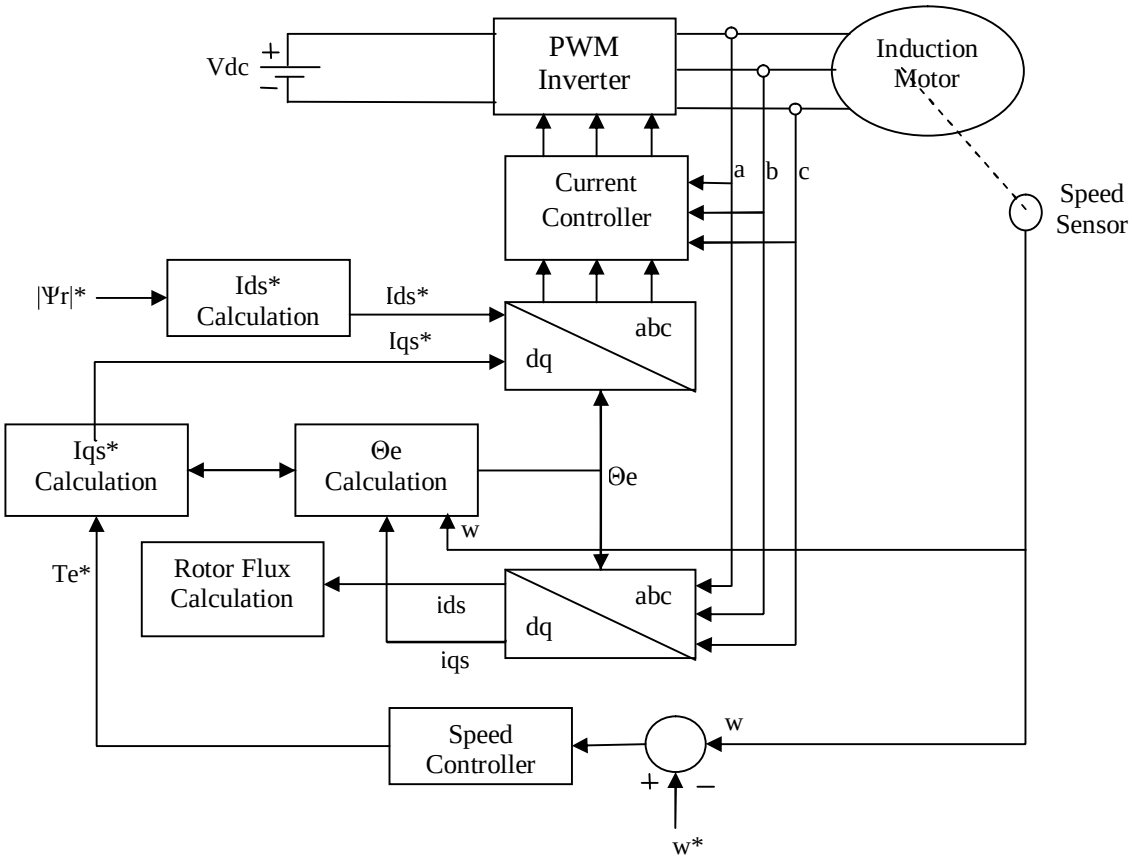

Figure 3.2 Block diagram of FOC scheme of induction motor drives.

A block diagram of field oriented control of induction motor drives is shown in figure 3..2. The induction motor is fed by a current- regulator. The speed control loop uses a PI controller to produce the quadrature axis current reference i_q* which controls the motor torque. The motor flux is controlled by the direct-axis current reference i_d*. Block d-q to abc is used to convert i_d* and i_q* into current references i_a*, i_b*, and i_c* for the current regulator.

d-q to abc Transformation

Consider a symmetrical three-phase induction machine with stationary as-bs-cs axes at 2π/3 angle apart. To transform the three-phase stationary reference frame (as-bs-cs) variable into two-phase stationary reference frame (d^s-q^s) variables and then transform these to synchronously rotating reference frame(d^e-q^e).and following transformation equations are used.

$$\begin{bmatrix} v_{as} \\ v_{bs} \\ v_{cs} \end{bmatrix} = \begin{bmatrix} cos\theta & sin\theta & 1 \\ \cos(\theta - 120°) & \sin(\theta - 120°) & 1 \\ \cos(\theta + 120°) & \sin(\theta + 120°) & 1 \end{bmatrix} \begin{bmatrix} v_{qs}^s \\ v_{ds}^s \\ v_{os}^s \end{bmatrix} \quad (3.11)$$

The corresponding inverse relation is given by equation (3.2)

$$\begin{bmatrix} v_{qs}^{s} \\ v_{ds}^{s} \\ v_{os}^{s} \end{bmatrix} = \frac{2}{3}\begin{bmatrix} cos\theta & \cos(\theta - 120°) & \cos(\theta + 120°) \\ sin\theta & \sin(\theta - 120°) & \sin(\theta + 120°) \\ 0.5 & 0.5 & 0.5 \end{bmatrix}\begin{bmatrix} v_{as} \\ v_{bs} \\ v_{cs} \end{bmatrix} \quad (3.12)$$

Where v_{os}^{s} is added as the zero sequence component, which may or may not be present. We have considered voltage as the variable. The current and flux linkage can be transformed by similar equations. Here θ is the angle of the orthogonal set α-β-0 with respect to any arbitrary reference .if the α-β-0 axes are stationary and the α axis is aligned with the stator a-axis,

then θ = 0 at all times, thus

$$\begin{bmatrix} v_{qs}^{s} \\ v_{ds}^{s} \\ v_{os}^{s} \end{bmatrix} = \frac{2}{3}\begin{bmatrix} 1 & -1/2 & -1/2 \\ 0 & \sqrt{3}/2 & \sqrt{3}/2 \\ 1/2 & 1/2 & 1/2 \end{bmatrix}\begin{bmatrix} v_{as} \\ v_{bs} \\ v_{cs} \end{bmatrix} \quad (3.13)$$

If the orthogonal set of reference rotates at the synchronous speed ω1, its angular position at any instant is given by equation (4.4)

$$\theta = \int_0^t \omega_1 \, t + \theta_0$$

(3.14)

The orthogonal set is then referred to as d- q- 0 axes. The three-phase rotor variables, transformed to the synchronously rotating frame, are

$$\begin{bmatrix} v_{qr}^{s} \\ v_{dr}^{s} \\ v_{or}^{s} \end{bmatrix} =$$

$$\frac{2}{3}\begin{bmatrix} \cos(\omega_e - \omega_r)t & \cos((\omega_e - \omega_r)t - 120°) & \cos((\omega_e - \omega_r)t + 120°) \\ sin(\omega_e - \omega_r)t & \sin((\omega_e - \omega_r)t - 120°) & \sin((\omega_e - \omega_r)t + 120°) \\ 0.5 & 0.5 & 0.5 \end{bmatrix}\begin{bmatrix} v_{as} \\ v_{bs} \\ v_{cs} \end{bmatrix}$$

(3.15)

It should be noted that the difference $\omega_e - \omega_r$ is the relative speed between the synchronously rotating reference frame and the frame attached to the rotor. This difference is also the slip frequency, ω_{sl}, which is the frequency of rotor.

θ_e Calculation Block

The rotor flux position θ_e required for coordinates transformation is generated from the rotor speed ω_m and slip frequency ω_{sl}.

$$\theta_e = \int (\omega_m + \omega_{sl}) dt \quad (3.16)$$

The slip frequency is calculated from the stator reference current i_{qs}* and the motor parameters.

$$\omega_{sl} = \frac{L_m}{|\psi_r|_{est}} \frac{R_r}{L_r} i_{qs}^* \quad (3.17)$$

I_{ds} Calculation Block

The stator direct-axis current reference i_{ds}* is obtained from rotor flux reference input $|\psi_r|$*

$$i_{ds}^* = \frac{|\psi_r|^*}{L_m} \quad (3.18)$$

I_{qs} Calculation Block

The stator quadrature-axis current reference i_{qs}* is calculated from torque reference T_e* as

$$i_{qs}^* = \frac{2}{3} \cdot \frac{2}{p} \cdot \frac{L_r}{L_m} \frac{T_e^*}{|\psi_r|_{est}} \quad (3.19)$$

Where L_r is the rotor inductance, L_m is the mutual inductance, and $|\psi_r|_{est}$ is the estimated rotor flux linkage.

3.3.3 Direct Torque Control of Induction Motor Drives

In a direct torque controlled (DTC) induction motor drives supplied by a voltage source inverter, it is possible to control directly the stator flux linkage *s* ψ (or the rotor flux *r* ψ or the magnetizing flux *m* ψ) and the electromagnetic torque by the selection of an optimum inverter voltage vector. The selection of the voltage vector of the voltage source inverter is made to restrict the flux and torque error within their respective flux and torque hysteresis bands and to obtain the fastest torque response and highest efficiency at every instant. DTC enables both quick torque response in the transient operation and reduction of the harmonic losses and acoustic noise. Simulation is the imitation of the operation of a real-world process or system over time. The act of simulating something first requires that a model be developed; this

model represents the key characteristics or behaviours/functions of the selected physical or abstract system or process.

Principle of Direct Torque Control (DTC)

The electromagnetic torque in the three phase induction machines can be expressed as follows.

$$te = \frac{3}{2} P \Psi s . is \quad (3.20)$$

Where ψ*s* is the stator flux, *is* is the stator current (both fixed to the stationary reference frame fixed to the stator) and P the number of pairs of poles. Equation (3.20) can be modified as equation (3.21).

$$te = \frac{3}{2} P |\Psi s| . |is| . \sin(\alpha s - \rho s) \quad (3.21)$$

Where ρs is the stator flux angle and αs is the stator current one, both referred to the horizontal axis of the stationary frame fixed to the stator. If the stator flux modulus is kept constant and the angle ρs is changed quickly, then the electromagnetic torque is directly controlled. The electromagnetic torque can also be given as equation (3.22).

$$te = \frac{3}{2} P \frac{Lm}{LsLr - Lm^2} |\Psi r| . |\Psi s| . \sin(\rho s - \rho r) \quad (3.22)$$

Because of the rotor time constant is larger than the stator one, the rotor flux changes slowly compared to the stator flux; in fact, the rotor flux can be assumed constant. (The fact that the rotor flux can be assumed constant is true as long as the response time of the control is much faster than the rotor time constant). As long as the stator flux modulus is kept constant, then the electromagnetic torque can be rapidly changed and controlled by means of changing the angle (ρs – ρr).

DTC Controller Design

The way to impose the required stator flux is by means of choosing the most suitable Voltage Source Inverter state. If the ohmic drops are neglected for simplicity, then the stator voltage

impresses directly the stator flux in accordance with the following equations.

$$\Delta\psi s = Vs . \Delta t \quad (3.23)$$

Decoupled control of the stator flux modulus and torque is achieved by acting on the radial and tangential components respectively of the stator flux-linkage space vector in its locus. These two components are directly proportional (Rs=0) to the

components of the same voltage space vector in the same directions. So imposing of proper voltage vector is important in direct torque control of induction motor. This we will obtained by using voltage source inverter.

Space Vectors

There are many topologies for the voltage source inverter used in DTC control of induction motors that give high number of possible output voltage vectors [16], [17] but the most common one is the six step inverter. A six step voltage inverter provides the variable frequency AC voltage input to the induction motor in DTC method. The DC supply to the inverter is provided either by a DC source like a battery, or a converter supplied from a three phase (or single phase) AC source. The inductor L is inserted to limit shot through fault current. A large electrolytic capacitor C is inserted to stiffen the DC link voltage.

The switching devices in the voltage source inverter bridge must be capable of being turned off and on. Insulated gate bipolar transistors (IGBT) are used because they have this ability in addition; they offer high switching speed with enough power rating. Each IGBT has an inverse parallel-connected diode. This diode provide alternate path for the motor current after the IGBT, is turned off. Each leg of the inverter has two switches one connected to the high side (+) of the DC link and the other to the low side (-); only one of the two can be on at any instant. When the high side gate signal is on the phase is assigned the binary number 1, and assigned the binary number 0 when the low side gate signal is on. Considering the combinations of status of phases a, b and c the inverter has eight switching modes (VaVbVc=000-111) two are zero voltage vectors V0 (000) and V7 (111) where the motor terminals is short circuited and the others are nonzero voltage vectors V1 to V6.

The dq model for the voltage source inverter in the stationary reference frame is obtained by applying the dq transformation Equation to the inverter switching modes. The six nonzero voltages space vectors will have the orientation shown in Figure 3.3, and also shows the possible dynamic locus of the stator flux, and its different variation depending on the VSI states chosen. The possible global locus is divided into six different sectors signalled by the discontinuous line. Each vector lies in the center of a sector of 60^{o} width named V1 to V6 according to the voltage vector it contains.

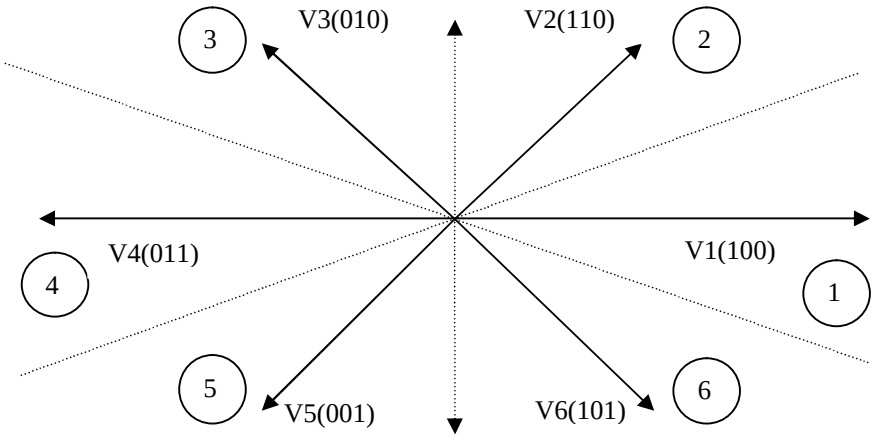

Figure 3.3 Switching voltage vectors and stator flux vector locus.

From equation (3.23) it can be seen that the inverter voltage directly force the stator flux, the required stator flux locus will be obtained by choosing the appropriate inverter switching state. Thus the stator flux linkage move in space in the direction of the stator voltage space vector at a speed that is proportional to the magnitude of the stator voltage space vector. By selecting step by step the appropriate stator voltage vector, it is then possible to change the stator flux in the required way [19]. If an increase of the torque is required then the torque is controlled by applying voltage vectors that advance the flux linkage space vector in the direction of rotation. If a decrease in torque is required then zero switching vector is applied, the zero vector that minimize inverter switching is selected. In summary if the stator flux vector lies in the k-th sector and the motor is running anticlockwise then torque can be increased by applying stator voltage vectors Vk+1 or Vk+2, and decreased by applying a zero voltage vector V0 or V7. Decoupled control of the torque and stator flux is achieved by acting on the radial and tangential components of the stator voltage space vector in the same directions, and thus can be controlled by the appropriate inverter switching. In general, if the stator flux linkage vector lies in the k-th sector its magnitude can be increased by using switching vectors Vk-1 (for clockwise rotation) or Vk+1 (for anticlockwise rotation), and can be decreased by applying voltage vectors Vk-2 (for clockwise rotation) or Vk+2 (for anticlockwise rotation). In Accordance with figure 3.3, the general table I can be written. It can be seen from table I, that the states Vk and Vk+3 , are not considered in the torque because they can both increase (first 30 degrees) or decrease (second 30 degrees) the torque at the same sector depending on the stator flux position.

Table I. GENERAL SELECTION TABLE FOR DIRECT TORQUE CONTROL.

Voltage Vector	Increse	Decrease
Stator Flux	V_k, V_{k+1}, V_{k-1}	V_{k+2}, V_{k-2}, V_{k+3}
Torque	V_{k+1}, V_{k+2}	V_{k-1}, V_{k-2}

Block diagram for the direct torque control scheme of induction motor is shown in figure 3.4.

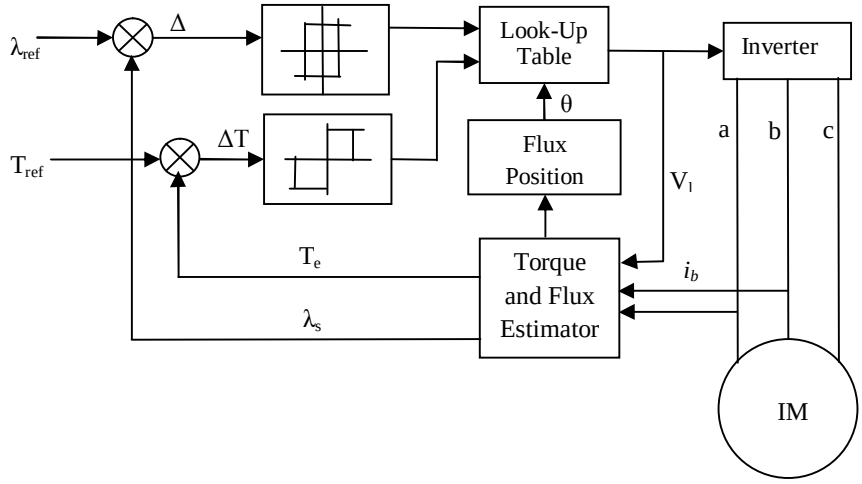

Figure 3.4 Block diagram of direct torque control of induction motor

As it can be seen, there are two different loops corresponding to the magnitudes of the stator flux and torque. The reference values for the flux stator modulus and the torque are compared with the actual values, and the resulting error values are fed into the two level and three-level hysteresis blocks respectively. The outputs of the stator flux error and torque error hysteresis blocks, together with the position of the stator flux are used as inputs of the look up table. The inputs to the look up table are given in terms of +1,0,-1 depend on whether the torque and flux errors within or beyond hysteresis bands and the sector number in which the flux sector presents at that particular instant.

3.4 Conclusion

In this chapter the speed controller design techniques are studied and described thoroughly. A framework of the field oriented or vector control and direct torque control of the induction motor drives is established. The flux and torque estimation blocks of FOC with the related equations are described. The switching table and the space vector for the DTC are explained.

CHAPTER 4
THREE PHASE CONTROLLED CONVERTER

CHAPTER 4
THREE PHASE CONTROLLED CONVERTER

4.1 Introduction

The non linear induction motor drives are responsible for harmonic distortion in power system. A nonlinear device is one in which the current is not proportional to the applied voltage. A harmonic is defined as a component with a frequency that is an integer multiple of the fundamental frequency. The harmonic number indicates the harmonic frequency: the first harmonic is the fundamental frequency (50 Hz), the second harmonic is the component with frequency two times the fundamental (100 Hz), and so on. AC drives in industries also posses the non linear performance when run without any harmonic and reactive power controller. A three phase controlled PWM converter design is proposed to control the harmonic generated by the induction motor drives in industries and also maintains unity power factor.

Ac drives used in industries have need of a variable-frequency supply that is taken from a converter–inverter arrangement. These ac drives usually use standard squirrel-cage induction motors because of their low price and maintenance. The ac side of inverter is connected to a load or to an ac system. The dc input to an inverter is a dc voltage source. A large capacitor or an LC filter with a small inductor and relatively large shunt capacitor connected to the output of the converter bridge gives the constant dc voltage output for inverters.

In order to generate the magnetic field motor produces harmonic currents. Harmonic currents can also be produced by the pitch of motor winding. Typical motor windings comprise 5–7 slots per pole, which causes the production of the fifth or seventh harmonic. In spite of the fact they are very small in magnitude than high harmonics in converter equipment; their existence is visible in the case of very large motors. The undesirable effects of harmonics are:

- Increased dielectric loss and heating of capacitors causes premature failure may draw excessive current.
- Interference with telecommunication systems, especially noise on telephone lines.

- Motors, transformers and switchgear can suffer from amplified losses and unnecessary heating.
- Induction motors may refuse to start (cogging) or may run at subsynchronous speeds.
- Circuit breakers may not succeed to interrupt currents due to inappropriate operation of blowout coils.

So, there is a need to rectify the problem of harmonic distortion caused by non linear industrial drives. A PWM converter is intended as a solution to the trouble of harmonic distortion in the following section. This converter is designed such that to keep a check and control the harmonic level and maintain the unity power factor.

4.2 Classification of Converters

Converters are power electronic systems that convert input ac power to output dc power. Converters come in many types and can be classified variedly as:

- Single-phase and three-phase
- Half-wave and full-wave
- Phase control and pulse width modulated
- Voltage source and current source converters

Single-phase vs. three-phase converters is a classification based on the type of ac input to the converter. The converters shown in Figure 4.1(a) and 4 .1(b) are diode converters.

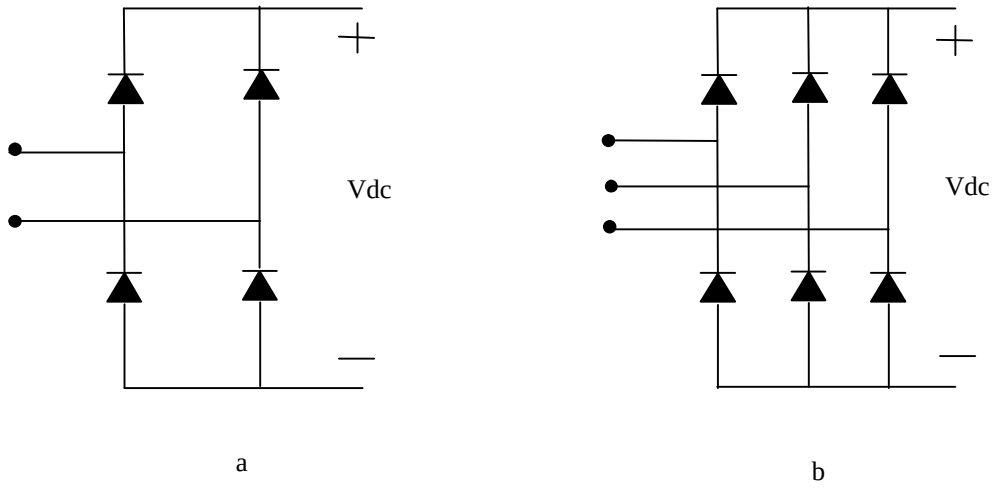

Figure 4.1 (a) Single-phase bridge rectifier (b) Three-phase bridge rectifier

The second classification is based on the rectification capability of the converter, full wave converter gives full rectified waveform in the output whereas half wave

converter gives half rectified waveform. The third classification relates to the type of semiconductor device used in the rectifier; uncontrolled rectifiers comprise of diodes as the switches, phase-controlled rectifiers comprise of SCR (silicon controlled rectifiers); and in pulse width modulated rectifiers; IGBT.s (insulated gate bipolar transistors) or power MOSFET.s (metal oxide field-effect transistors) are used. The rectifier is switched using pulses that are generated using sine-triangle or space vector pulse width modulation.

The pulse-width modulated converters can be further divided on the basis of the relationship between the ratios of the input and output voltages. Some examples of the pulse-width modulated converters are buck, boost, and buck-boost converters. In buck converters, the dc output voltage is lower in magnitude than the peak value of the ac input. Similarly, the boost converter has an output dc voltage that is higher in magnitude than the peak value of the ac input voltage. The buck-boost converter can have an output voltage, either lower or higher in magnitude when compared to the ac input, with the duty ratio of the switches determining the nature of the output. The fourth classification is voltage source and current source

4.2.1 Voltage Source Converter

The converter whose input is the fixed voltage source represents the voltage source converter (VSC). VSC are further classified as PWM converter and square wave converter. In PWM converters the output voltage is obtained by pulse width modulating of the converter switches and hence these converters are called PWM converters. In square wave converter the input voltage controls only the frequency of the output voltage, this output voltage has waveform similar to square wave and hence the name square wave voltage source converter.

4.2.2 Current Source Converter

In a Current Source Converter (CSC), the DC current is kept constant with a small ripple using a large inductor, thus forming a current source on the DC side. The direction of power flow through a CSC is determined by the polarity of the DC voltage while the direction of current flow remains the same.

4.3 Three Phase PWM Converter Modelling

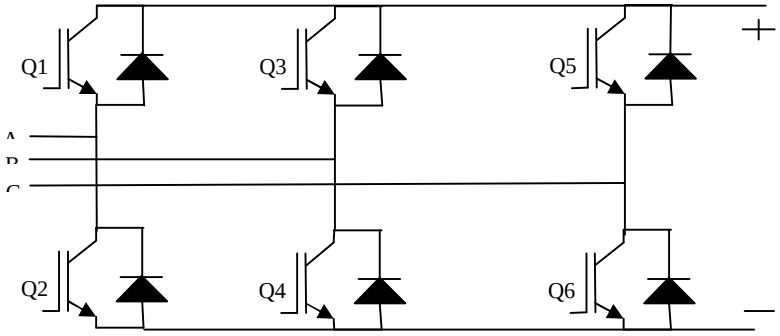

Figure 4.2 Topology for three phase PWM converter

Figure 4.2 shows basic diagram of the three-phase converter where A, B, C are the three phase, 50Hz supply voltage.

This topology of three phase converter regulates DC output voltage while offering low distortion to the line current [27]. Thus converter gives near sinusoidal current waveform and maintain power factor to unity.

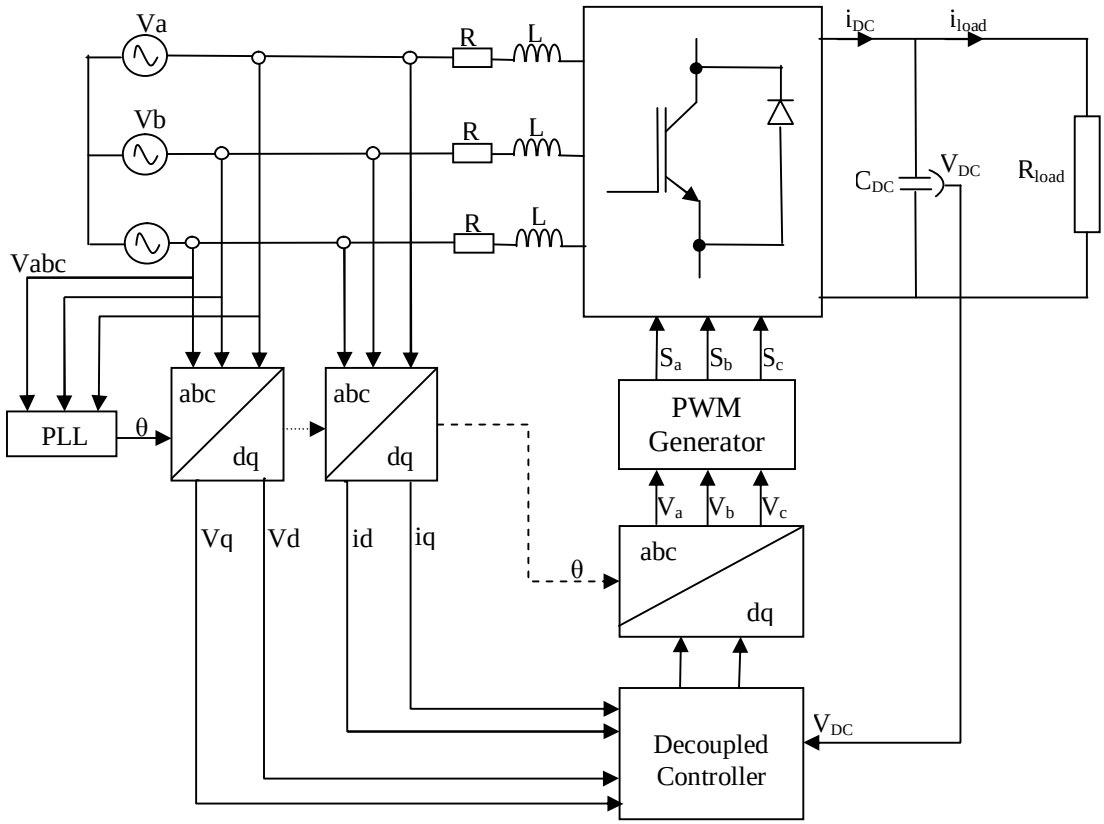

Figure 4.3 Block diagram of PWM converter control scheme

In figure 4.3 the block diagram of the PWM converter control scheme is shown. According to the proposed scheme the line voltage Vabc is fed to the phase locked loop block. PLL calculates the voltage angle θ and is then sent to the abc to dq transformation blocks. This transformation block transforms line currents and voltages to the stationary components dq.

Secondly, the dq-coordinate values and the DC-link voltage value are fed to a decoupled controller. Finally, the reference voltages created by the controller are sent to the PWM block (Pulse Width Modulation) to create the switching patterns Sa, Sb and Sc. Accordingly the control scheme of PWM converter has three sub parts: the PLL, a decoupled controller composed by a current and voltage controller and a PWM block.

PLL: Phase Locked Loop

The Phase-Locked Loop (PLL) block is a feedback control system that automatically adjusts the phase of a locally generated signal to match the phase of an input signal. This block is most appropriate when the input is a narrowband signal. This PLL has three components: A multiplier used as a phase detector, filter and VCO. The filter's transfer function is specified using the lowpass filter numerator and lowpass filter denominator parameters. Each is a vector that gives the respective polynomial's coefficients in order of descending powers of s. To design a filter, functions such as butter, cheby1, and cheby2 in Signal Processing Toolbox software are used.

In voltage-controlled oscillator (VCO) the characteristics of the VCO are specified as the VCO quiescent frequency, VCO initial phase, and VCO output amplitude parameters. The input signal represents the received signal. The input must be a sample-based scalar signal. The three output ports produce: The output of the filter, The output of the phase detector, The output of the VCO

Current Controller:

A summary for controller design based on Internal Model Control (IMC) with synchronous PI control (decoupled controller) is explained in this section [32]. To make the following more understandable, a first schematic for decoupled controller is given Figure 4.4 with the current controller.

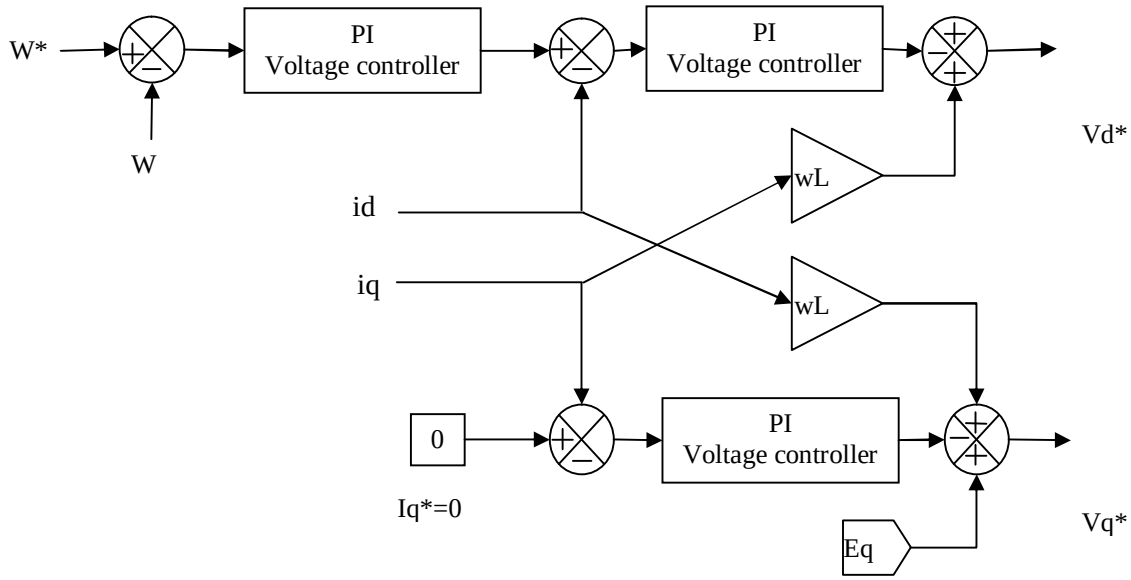

Figure 4.4 Block diagram decoupled controller.

PI controllers are inherently incapable of giving zero steady state control error for a sinusoidal reference. The integral action removes the error only if the reference value is constant in steady state. Using Clarke and Park transformations, the current measurements are transformed to DC quantities and are then sent to a PI controller for the results. Main qualities for dq-frame current controller are: rapid dynamic response, good precision in current tracking and less sensitivity to parameter deviations.

In this system, the line current iL is split into a q-component iq and a d-component id. id determines the active power flow whereas iq the reactive power. The unity power factor condition is established when the line current vector iL is arrange in a line with line voltage uL. Furthermore, the equation for power shows that the reactive power is set to zero.

$$P = \frac{3}{2} Re\{vdq(idq)*\} = \frac{3}{2}(vdid + vqiq) = \frac{3}{2}(Edid + Eqiq) \quad (4.1)$$

$$Q = \frac{3}{2} Im\{vdq(idq)*\} = \frac{3}{2}(vdid - vqiq) = \frac{3}{2}(Edid - Eqiq) \quad (4.2)$$

Now if we set the reference iq to zero and we know that the line voltage vector is aligned with the daxis, so Eq= 0 V. Finally, we get

$$P = \frac{3}{2} Ed\ id \quad (4.3)$$

$$Q = 0 \quad (4.4)$$

PWM (Pulse Width Modulation) Block:

Sinusoidal waveform is modulated with the use of a triangular carrier signal [33]. The idea is to compare three sinusoidal reference voltages Ua*, Ub* and Uc* to the triangular waveform. By comparison, the logical signals Sa, Sb and Sc, which characterize switching instants of the power transistor, are generated. Voltage harmonics are concentrated around switching frequency and multiple of switching frequency by operation with constant carrier signal.

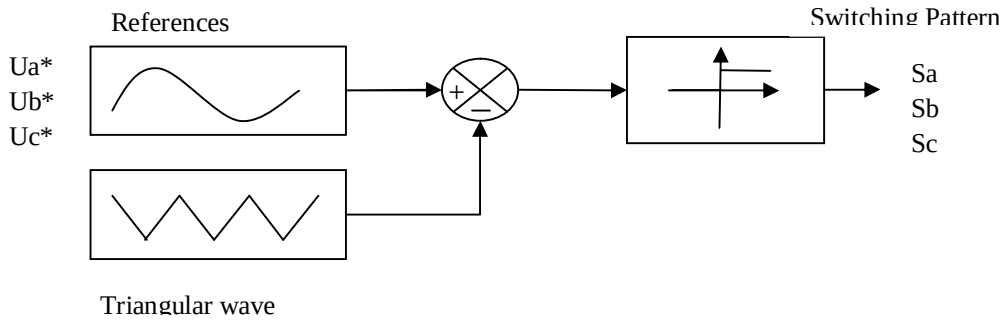

Figure 4.5 Diagrammatic representation of sinusoidal pulse width modulation technique

In a digital current control system, the current is sampled with time interval Ts. To avoid electromagnetic interference (EMI) due to ON/OFF switching of the valves, it is useful to synchronize the sampling with converter switching. Current samplings are taken in between switching. These samplings coincide with the positive and negative peak values of the triangular waveform.

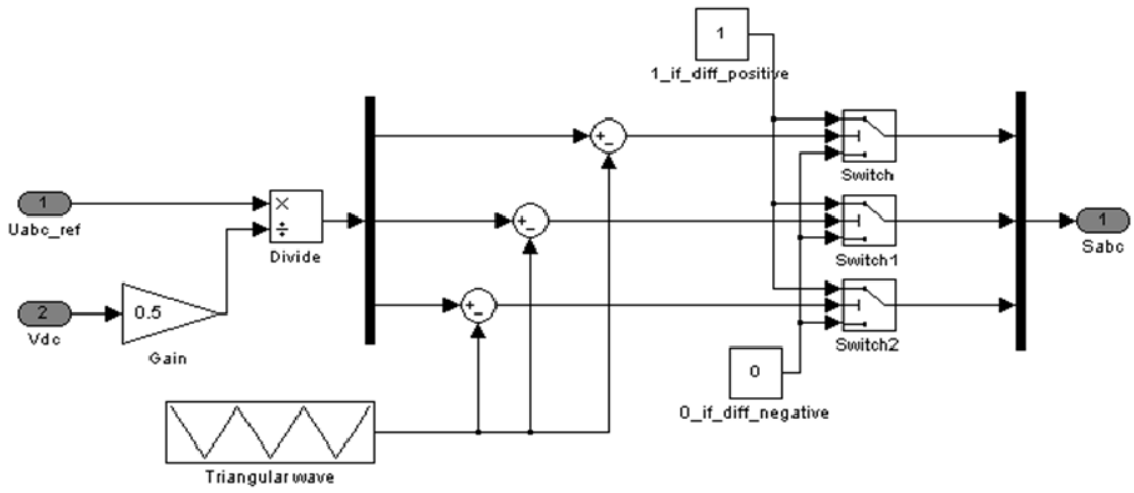

Figure 4.6 Simulink PWM Block Diagram

Using synchronous sampling, approximately the mean value of the current is obtained. Thus, not only EMI is avoided, but also the current ripple is reduced.
The amplitude of triangular wave should be Vdc/2. But Vdc is not constant in our case. We should first normalized the reference value by Vdc/2 and compare this value with a triangular wave with an amplitude of 1. The following figure 4.6 shows the Simulink block diagram.

4.4 Conclusion

The PWM ac to dc converter is designed to implement for controlling harmonic distortion and reactive power. The current controller technique is described with the help of block diagrams. PWM generator block is explained which is employed for the production of pulse width modulated waveforms. The chapter concludes the complete design methodology of the three phase PWM converter.

CHAPTER 5
MATLAB/SIMULINK MODELS OF INDUCTION MOTOR DRIVES

CHAPTER 5
MATLAB/SIMULINK MODELS OF INDUCTION MOTOR DRIVES

5.1 Introduction

A computer simulation is an effort to model a real-life or hypothetical condition on a computer so that it can be premeditated to see how the system works. By simply changing variables in the simulation, predictions can be made about the behaviour of the system. Simulation is a tool to virtually investigate the behaviour of the system.

The simulation blocks of PWM converter, direct torque control of industrial drives and field oriented control of industrial drives are shown in the following sections.

5.2 PWM Converter Simulation Blocks

The sub-blocks of PWM converter are PWM Generator, Current Controller, and Phase Locked Loop are shown in figure 5.1. Where Vabc is the three phase voltages and Iabc are the three phase currents.

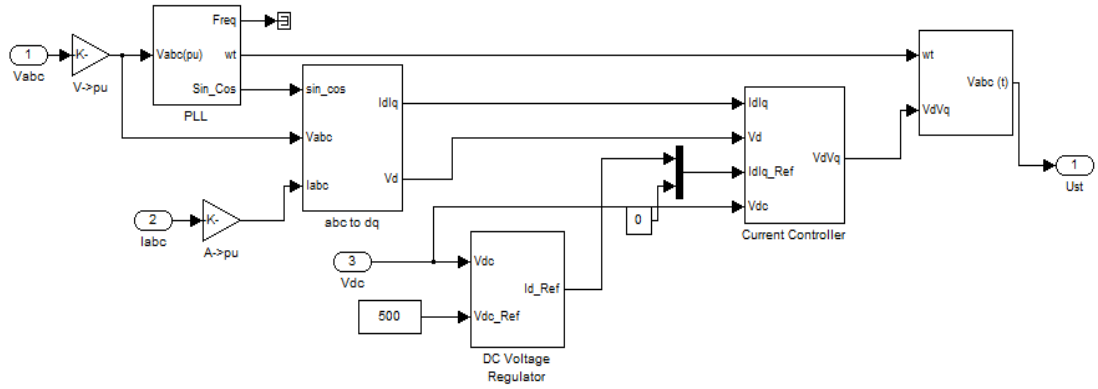

Figure 5.1 Controller sub block of the converter.

PWM Generator

The PWM Generator block generates pulses for carrier-based pulse width modulation (PWM) converters using two-level topology. The pulses are generated by comparing a triangular carrier waveform to a reference modulating signal. The

modulating signals can be generated by the PWM generator itself, or they can be a vector of external signals connected at the input of the block. One reference signal is needed to generate the pulses for a single- or a two-arm bridge, and three reference signals are needed to generate the pulses for a three-phase. The following figure 5.2 shows the PWM generator simulation block diagram.

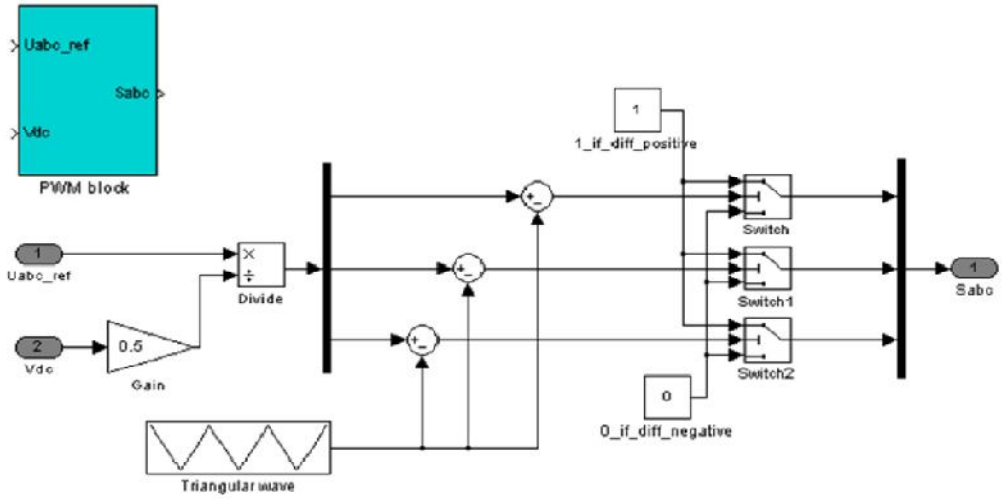

Figure 5.2 Simulation block of PWM generator

Current Controller

In current controller internal model control method for controller design is used, for which the resulting controller becomes directly parameterized in terms of the plant model parameters and gives the desired closed-loop bandwidth. Figure 5.3 gives the simulation block diagram of the current controller used in the converter.

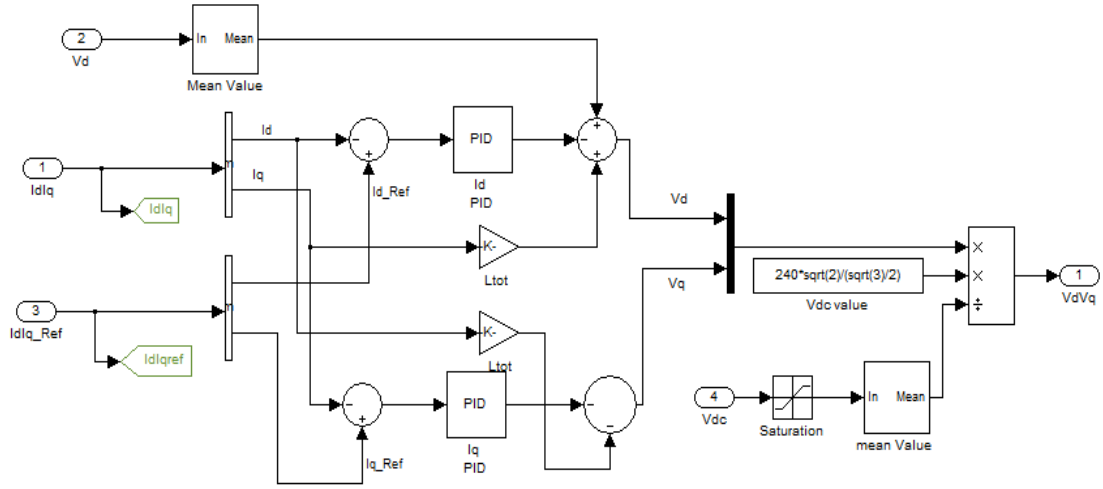

Figure 5.3 Current controller block of converter

Phase Locked Loop (PLL)

Phase-locked loop is implemented to recover phase of the input signal. Due to the feedback control system of Phase-Locked Loop (PLL) block, it deliberately adjusts the phase of a locally generated signal to match the phase of an input signal. This block is most appropriate when the input is a narrowband signal. Figure 5.4 shows the block diagram of PLL used in converter.

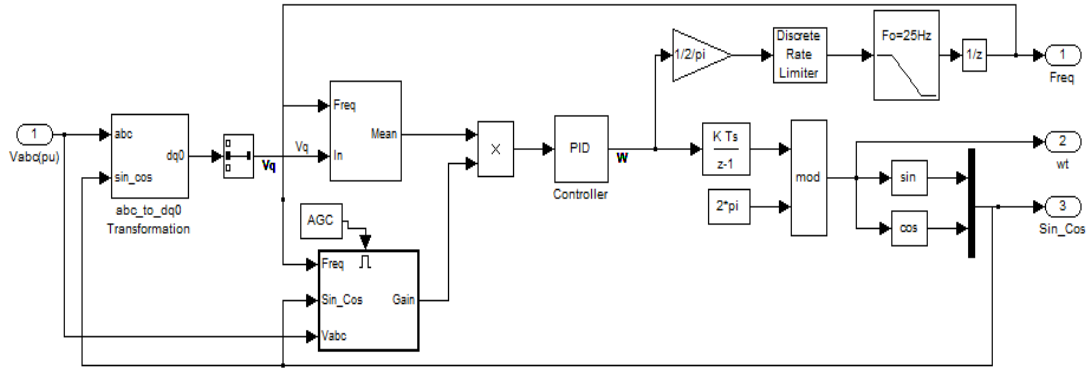

Figure 5.4 Phase locked loop block of converter

5.3 Direct Torque Control Scheme

Various sub blocks of direct torque control are explained below.

Direct Torque Control Sub-block

The simulation block diagram of the direct torque control of induction motor drives is shown in figure 5.5. This block diagram consists of sub-blocks of flux and torque estimator, hysteresis controller and speed controller.

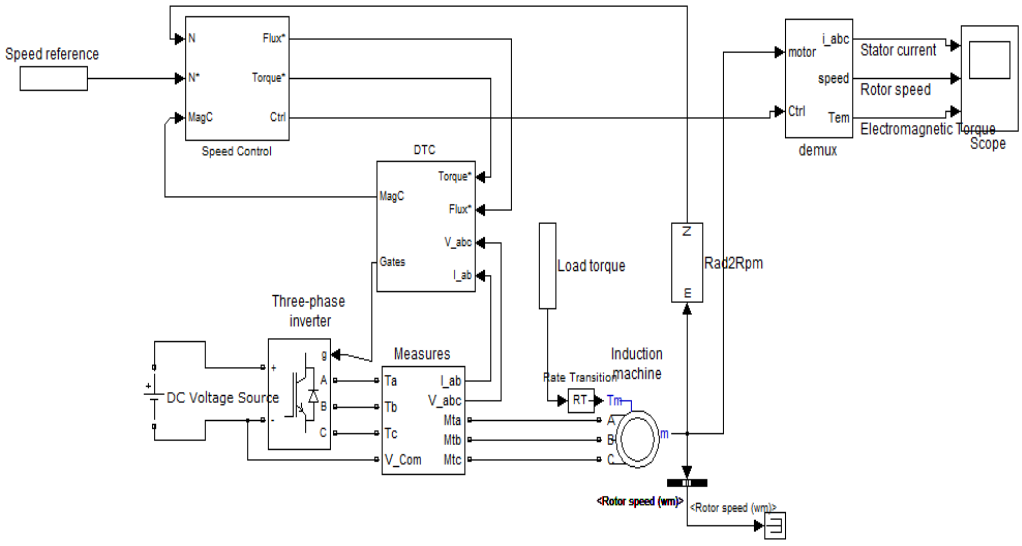

Figure 5.5 Simulink model of DTC of induction motor

Torque and flux estimator in simulink/matlab environment

The electromagnetic torque depends on the stator currents and the linkage fluxes. The stator currents are measurable quantities. There is electronic equipment that measures the current with great accuracy.

Most of the flux estimation techniques proposed is based on voltage model, current model, or the combination of both. The estimation based on current model normally applied at low frequency, and it requires the knowledge of the stator current and rotor mechanical speed or position. The use of rotor parameters in the estimation introduced error at high rotor speed due to the rotor parameter variations. So in this present DTC control scheme the flux and torque are estimated by using voltage model described by equations (5.1- 5.3), which does not need a position sensor and the only motor parameter used is the stator resistance.

$$\Psi_{sD} = \int (VsD - RsIsD)dt = isD.\frac{Lx}{Lm} + \Psi_{rd}.\frac{Lm}{Lr} \quad (5.1)$$

$$\Psi_{sQ} = \int (VsQ - RsIsQ)dt = isQ.\frac{Lx}{Lm} + \Psi_{rq}.\frac{Lm}{Lr} \quad (5.2)$$

Where Lx = Ls.Lr-Lm² and isD, isQ are calculated by using equations 5.1 and 5.2. And torque can be estimated by equation 5.3

$$te = \frac{3}{2} P(\Psi sD . isQ - \Psi sQ. isD) \quad (5.3)$$

By using these estimated values from voltage model we proceed to the lookup table to select the proper voltage vector. The torque and the flux estimator is formulated based on equation (5.3) and in the Simulink/Matlab environment it can be designed as in figure 5.6.

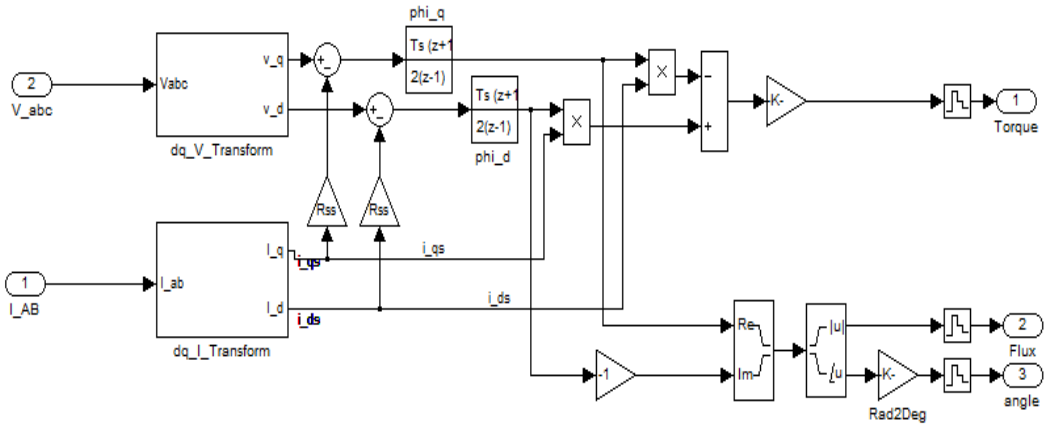

Figure 5.6 Torque and flux estimator simulink block

Flux and Torque Hysteresis Controller

The torque and flux regulator, which consists of one hysteresis controller, is built with Simulink blocks. The motor actual flux and torque are provided by the measurement output of the Asynchronous Machine block. The actual motor flux and torque are compared in hysteresis type relay with reference flux and torque. The torque and flux regulator are shown in figure 5.7.

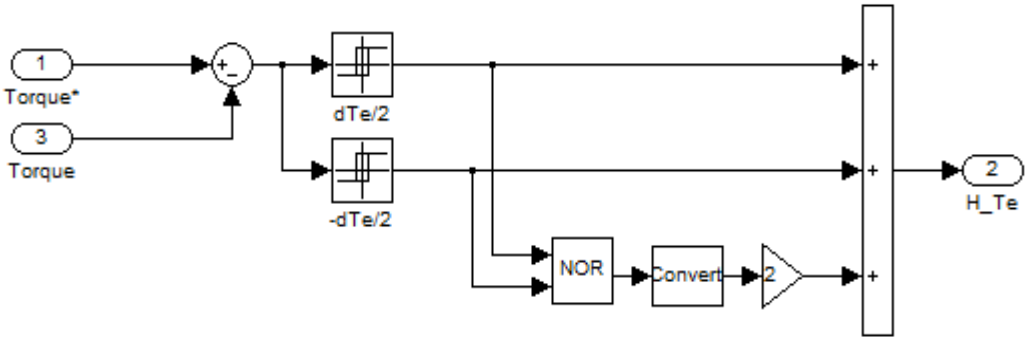

Figure 5.7 Flux and Torque hysteresis controller

Speed Controller

The rotor speed is compared with the reference speed of the induction motor in the speed controller block as shown in the block diagram.

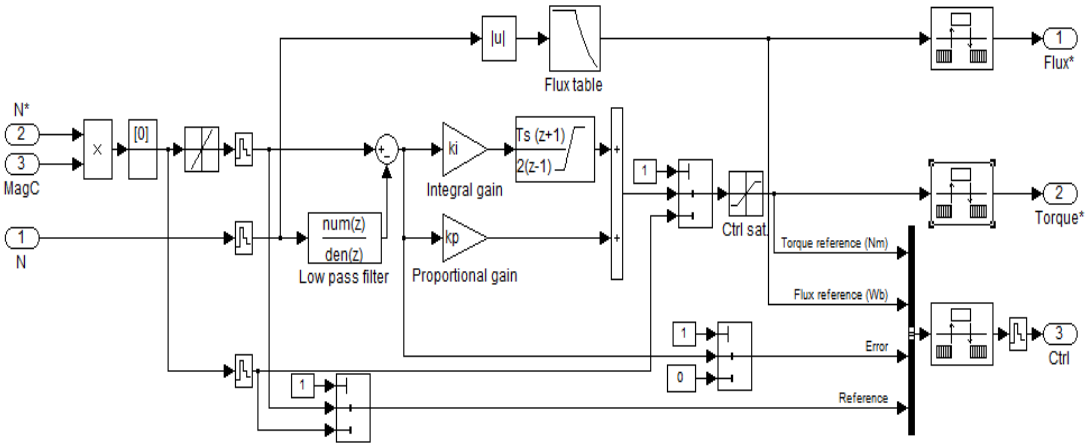

Figure 5.8 Speed controller subsystem of Direct torque control of induction motor

The subsystem contains standard blocks of proportional gain, integral gain and filter as shown in figure 5.8. The three generated signals flux, torque and control (ctrl) are passed to DTC block of the system.

5.4 Field Oriented Control Scheme

Various sub blocks of field oriented control scheme are shown below.

Field Oriented Control Sub Block

Figure 5.9 shows the MATLAB model of the indirect vector control induction motor drives. The induction motor is modeled by an asynchronous machine block.

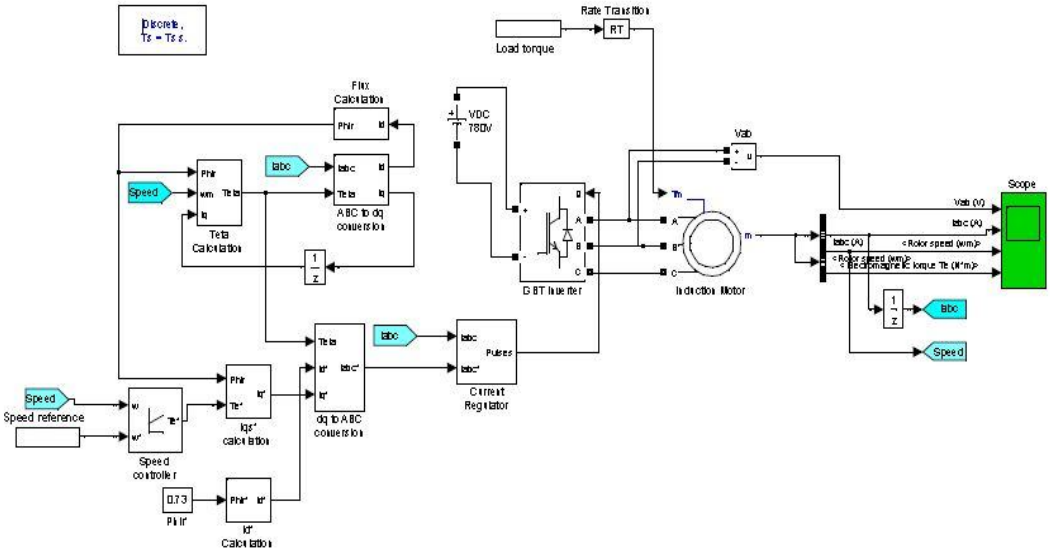

Figure 5.9 Matlab Simulink block diagram of FOC scheme.

Hysteresis Current Regulator

The current regulator, which consists of three hysteresis controllers, is built with Simulink blocks as shown in figure 5.10. The motor actual currents are provided by the measurement output of the Asynchronous Machine block. The actual motor currents and reference current are compared in hysteresis type relay.

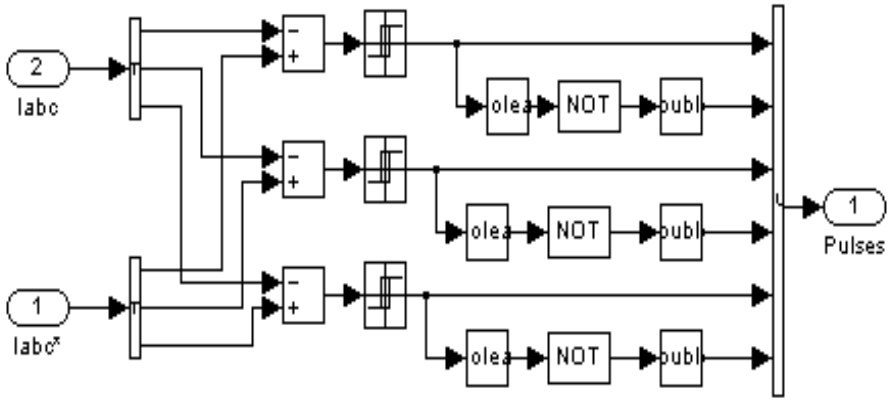

Figure 5.10 Hysteresis current regulator block

Flux Calculation Block

The rotor flux is calculated by the flux calculation block as shown in fig 5.11.

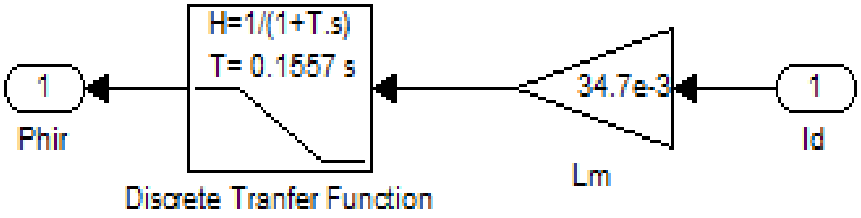

Figure 5.11 Block for Flux Calculation

Lr = Ll'r +Lm = 0.8 +34.7= 35.5 mH

Lm = 34.7 mH

Tr = Lr / Rr = 0.1557 sec

Rr = 0.228 Ω

Phir = Lm *Id / (1 +Tr .s)

Theta Calculation Block

The rotor flux position (θ_e) is calculated by the Theta Calculation Block shown in figure 5.12.

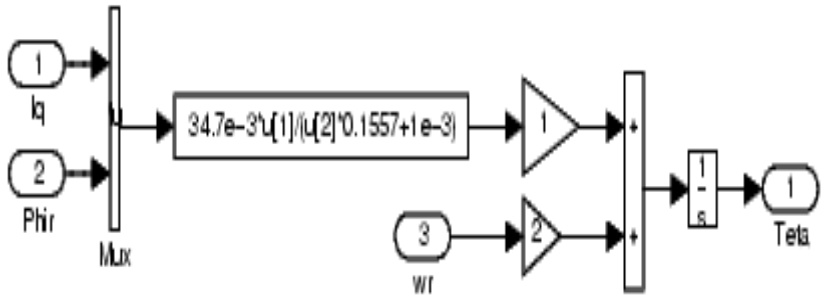

Figure 5.12 Block for Theta Calculation

d-q to abc Transformation Blocks

The conversions between abc and dq reference frames are executed by the dq to abc transformation blocks. The dq to abc transformation block is shown in figure 5.13.

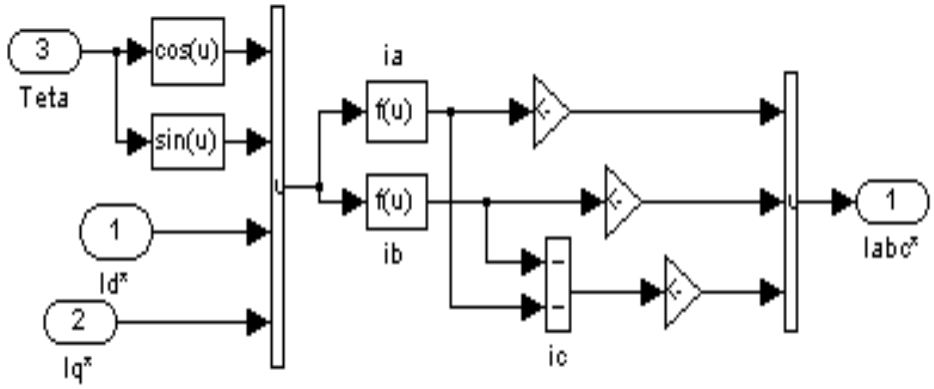

Figure 5.13 Transformation block: d-q to abc

abc to d-q Transformation Blocks

The conversions between abc and dq reference frames are executed by the abc to dq transformation blocks. The abc to dq block is shown in figure 5.16.

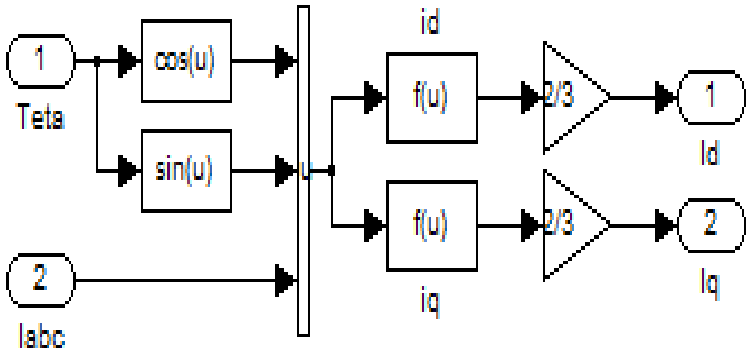

Figure 5.14 Transformation Blocks: abc to d-q

5.5 Conclusion

The simulation diagrams of the complete system are shown with sub blocks of each technique of control. The PWM converter blocks with the sub blocks of current controller, PLL and PWM generator are shown. The PWM converter with DTC and FOC controller's block diagram are shown. All the sub systems of FOC and DTC simulation block diagrams are explained. The simulation results of 50 hp induction motor drives are shown for different loads and speeds.

CHAPTER 6
SIMULATION RESULTS

CHAPTER 6
SIMULATION RESULTS

6.1 Simulation and Results

In this work the performance of field oriented and direct torque control of industrial induction motor drives. Simulation has been performed on MATLAB R2007a on Intel Core 2 Duo Processor 2.4 GHz. Window7 Home basic (64-bit) Laptop. The speed, currents and torque were recorded for load and no load and 50% of full load.

In order to show field oriented and direct torque control of industrial induction motor drives designed using hysteresis current algorithm, the simulation has been carried out on the 3-phase, 200hp, 480V squirrel cage induction motor with reference speed 150 rad/sec.

This vector controlled drives is further fed from a PWM converter. This converter provides smooth DC voltage to the inverter of the induction motor. The converter is supplied from three phase 50Hz, 415V supply.
The DC voltage output of the converter is applied to the inverter input of the two control schemes. This Vdc i.e DC-link voltage of the system is shown in figure 6.1.

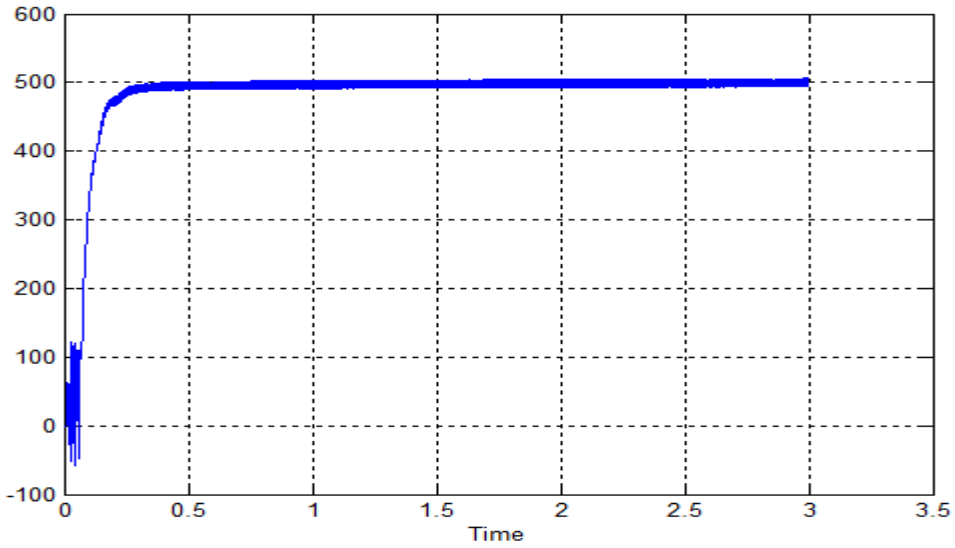

Figure 6.1 DC link voltage output of the PWM converter of the system

The converter gives 490V approximately. This dc voltage is sent to the inverter. Induction motor rated voltage is 480V, so this dc link voltage matches with the drives rating.

6.2 Results of DTC Scheme

Source voltage and current for DTC scheme for induction motor with three phase PWM converter are shown in figure 6.2.

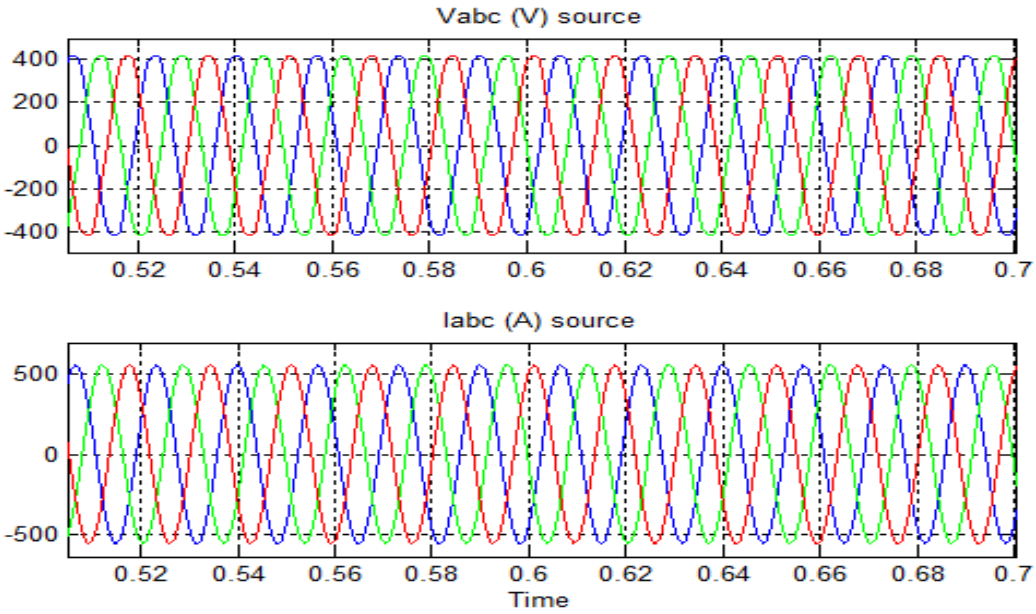

Figure 6.2 Source current and voltage waveform of three phase PWM converter

The source current and source voltage for DTC type of control scheme are shown coinciding to confirm the unity power factor in figure 6.3.

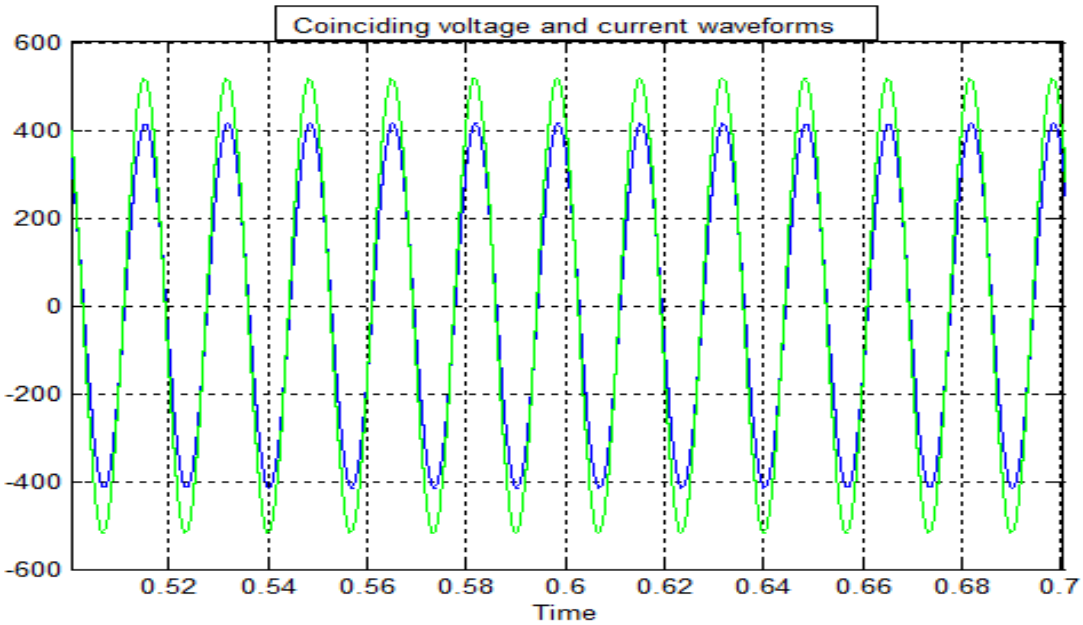

Figure 6.3 Unity power factor waveform for DTC

6.2.1 DTC Scheme Results at Different Loads

The no load, half load and full load performance characteristics of direct torque control of induction motor drives are shown in the following figures 6.4, figure 6.5, figure 6.6. Figure 6.4 shows no load characteristics at rated speed of 150 rad/sec. Figure 6.5 shows half load characteristics and figure 6.6 shows full load characteristics.

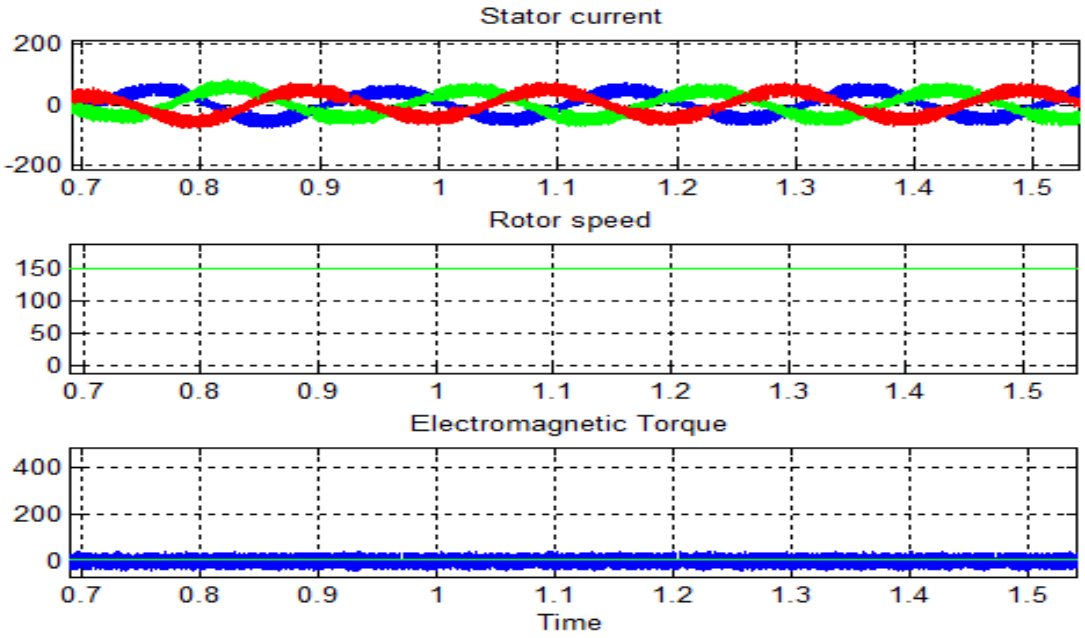

Figure 6.4 Simulink plot showing stator currents, rotor speed and electromagnetic torque for no load condition at speed of 150 rad/sec.

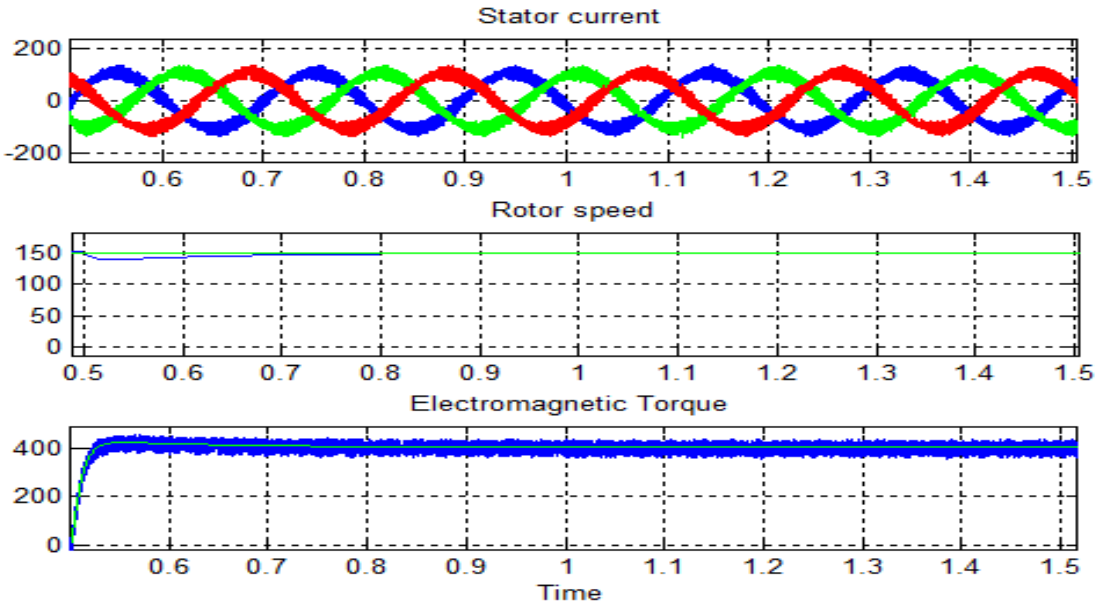

Figure 6.5 Simulink plot showing stator currents, rotor speed and electromagnetic torque for half load condition at speed of 150 rad/sec.

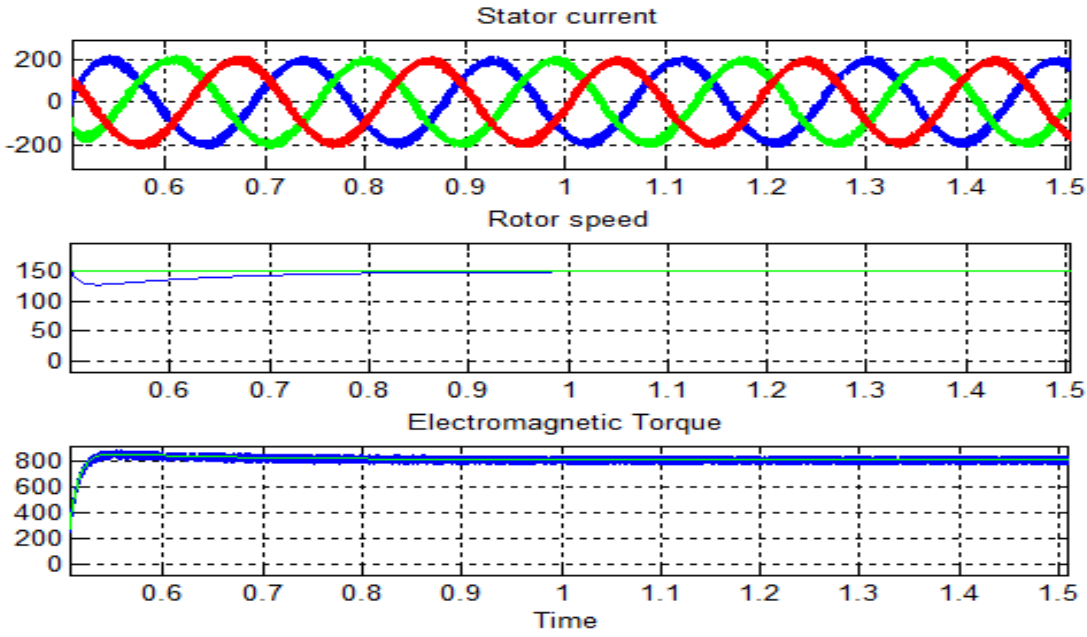

Figure 6.6 Simulink plot showing stator currents, rotor speed and electromagnetic torque for full load condition at speed of 150 rad/sec.

6.2.2 DTC Scheme Results at Different Speeds

The stator current, rotor speed and electromagnetic torque of direct torque control scheme for different speeds is shown in the following figures. Figure 6.7 shows the full load torque results at a speed of 50rad/sec, figure 6.8shows results at 100rad/sec, figure 6.8 shows results at 150rad/sec and figure 6.9 shows results at 200rad/sec.

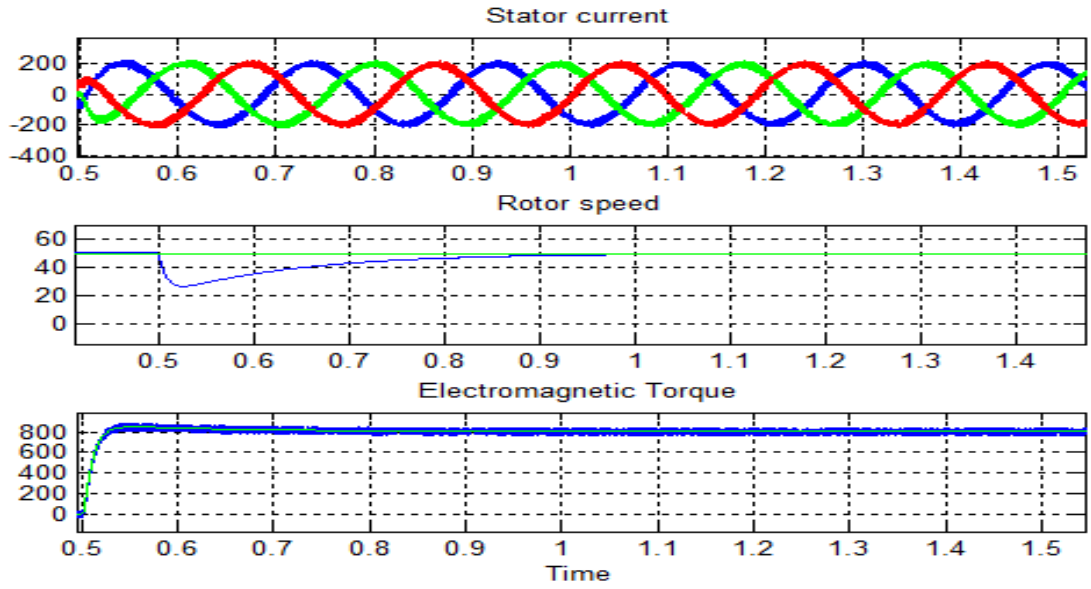

Figure 6.7 Simulink plot for DTC scheme showing three phase stator current, speed and electromagnetic torque for full load (800Nm) at 50rad/sec speed

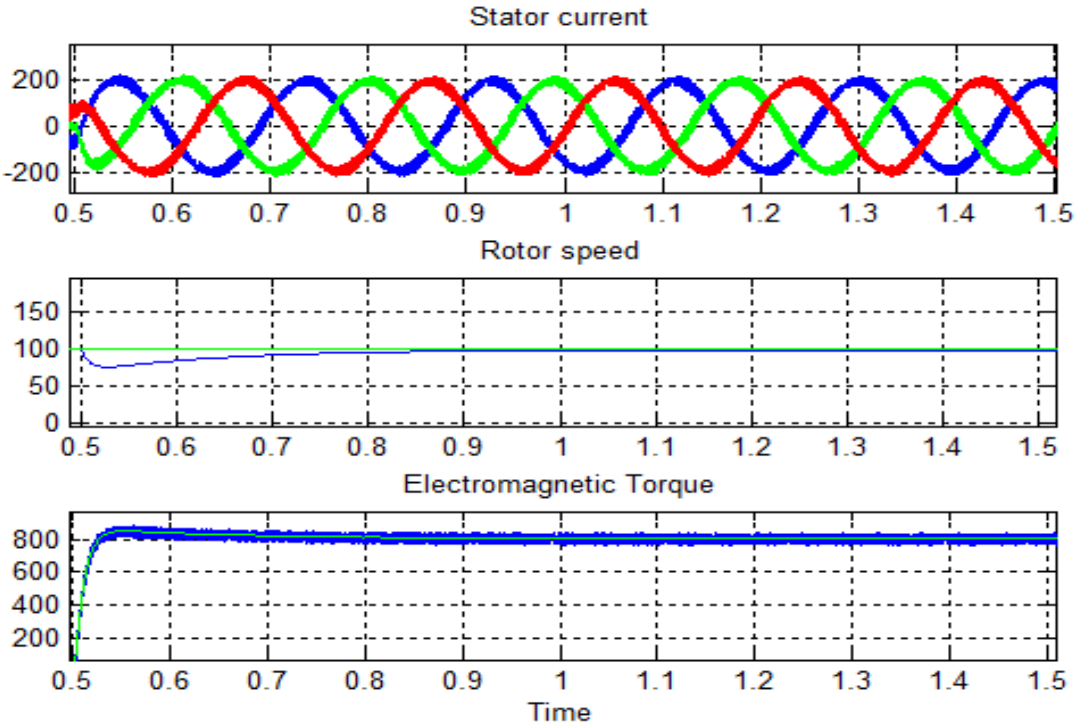

Figure 6.8 Simulink plot for DTC scheme showing three phase stator current, speed and electromagnetic torque for full load (800Nm) at 100rad/sec speed

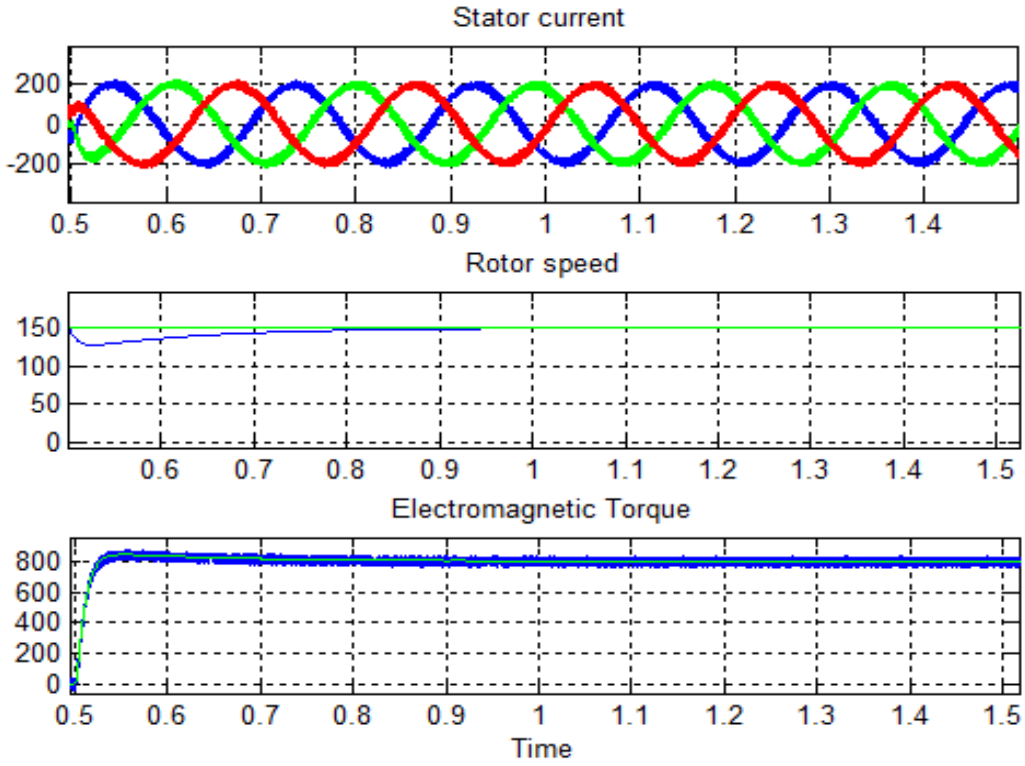

Figure 6.9 Simulink plot for DTC scheme showing three phase stator current, speed and electromagnetic torque for full load (800Nm) at 150rad/sec speed

6.3 Results of FOC Scheme

Three supply current and voltage for full load of FOC scheme are shown in figure 6.10.

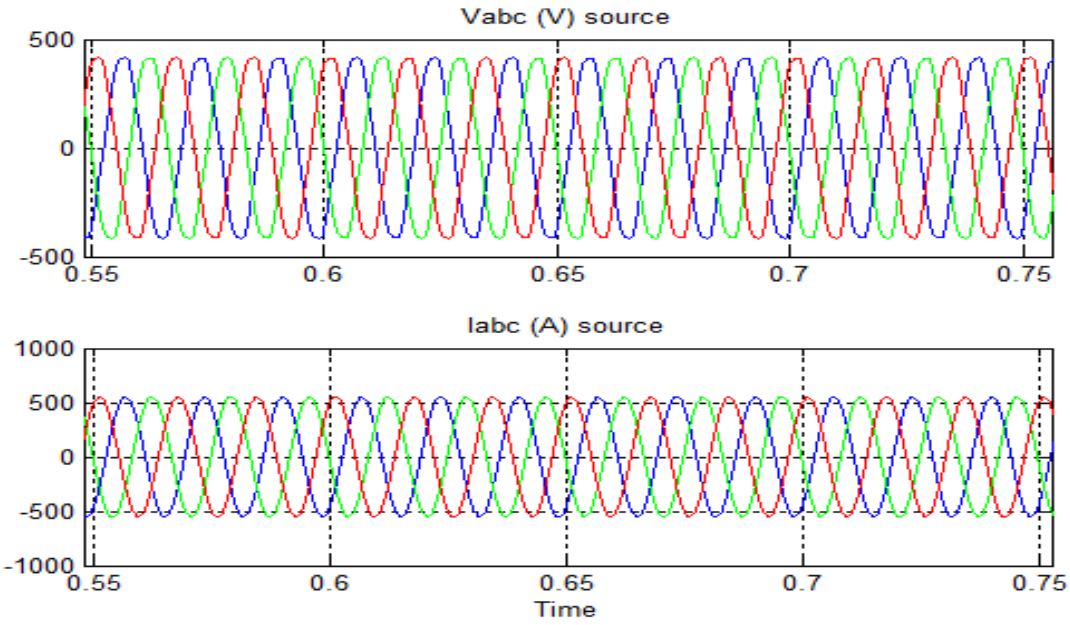

Figure 6.10 Source current and voltage waveform of three phase PWM converter

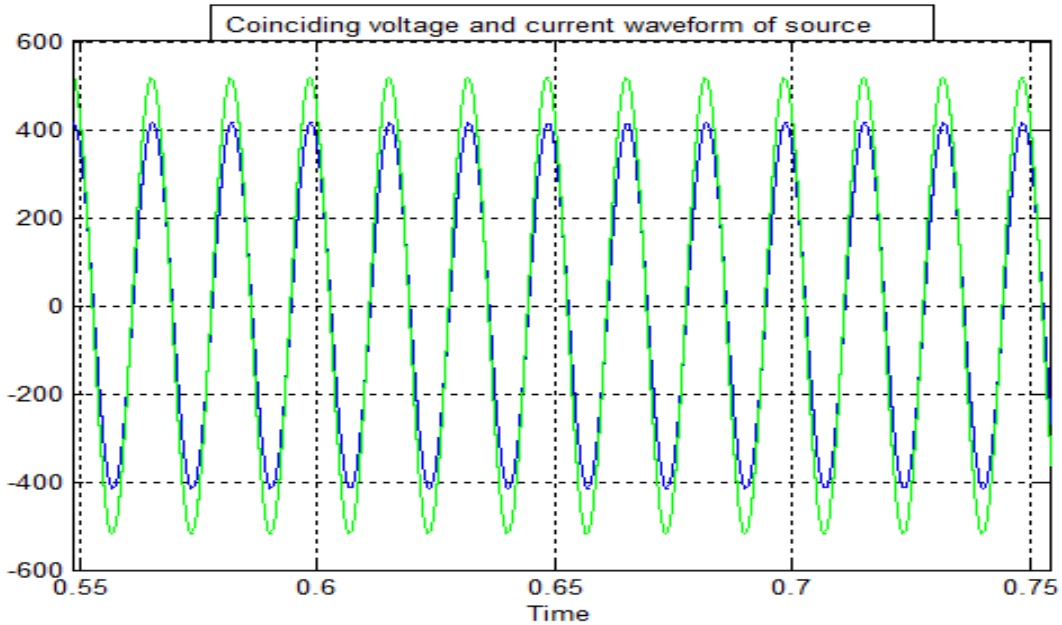

Figure 6.11 Unity power factor waveform of FOC

Figure 6.11 shows the current and voltage waveform alignment to confirm unity power factor for the FOC scheme for induction motor.

6.3.1 FOC Scheme Results at Different Loads

The no load, half load and full load performance characteristics of field oriented control of induction motor drives are shown in the following figures 6.12, figure 6.13, figure 6.14. Figure 6.12 shows no load characteristics at rated speed of 150 rad/sec. Figure 6.13 shows half load characteristics and figure 6.14 shows full load characteristics. The full load torque is 800Nm and half load torque is 400Nm.

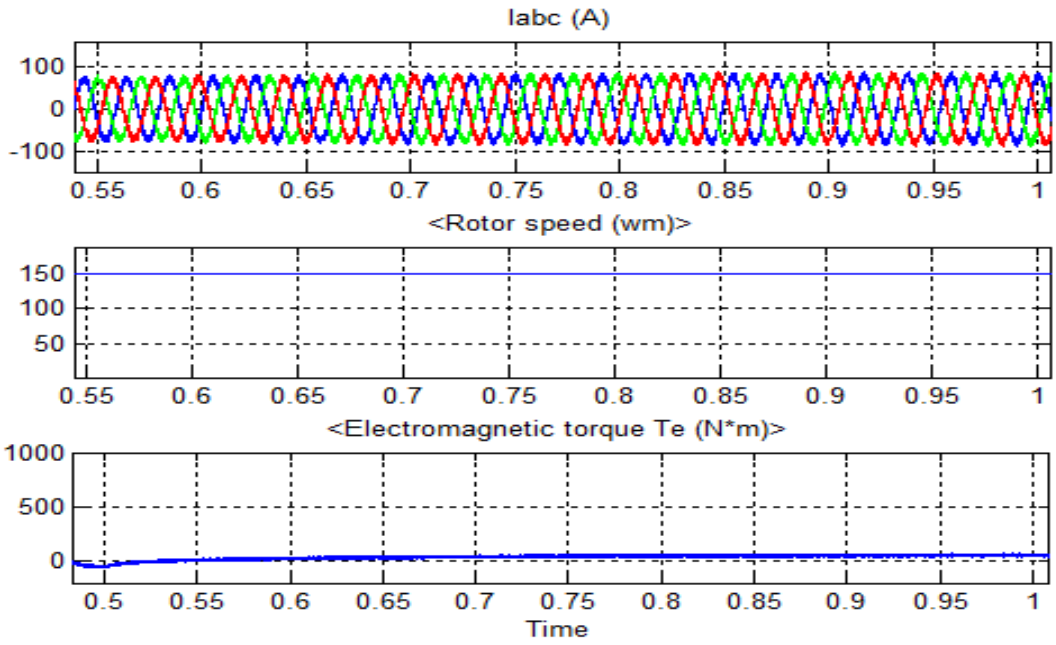

Figure 6.12 Simulink plot showing three phase stator current, speed and electromagnetic torque on no load at 150rad/sec speed.

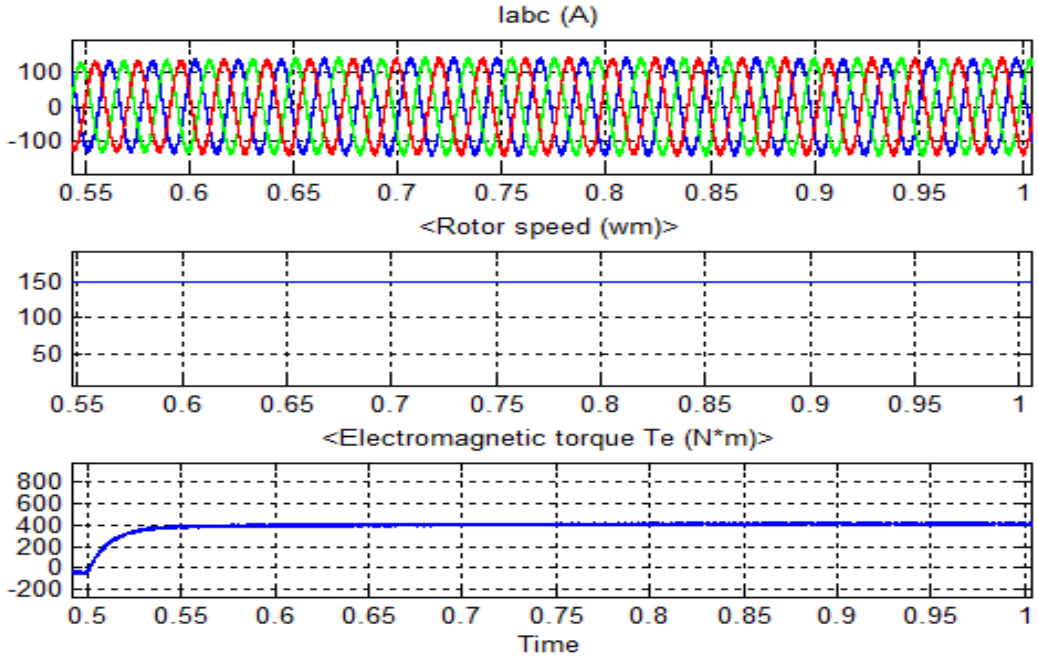

Figure 6.13 Simulink plot showing three phase stator current, speed and electromagnetic torque on half load at 150rad/sec speed.

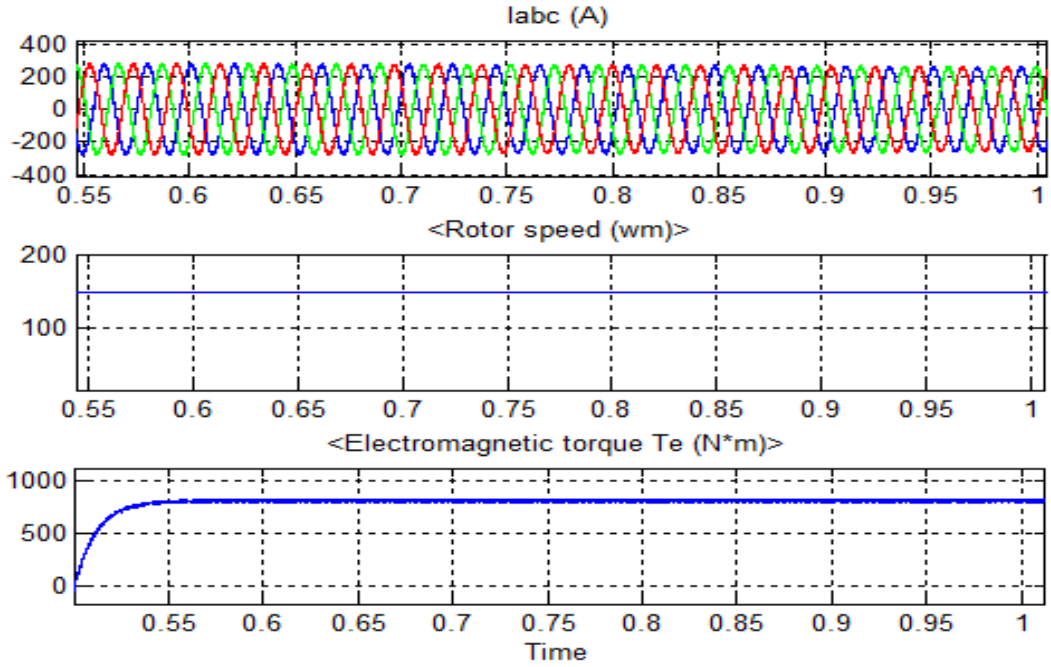

Figure 6.14 Simulink plot showing three phase stator current, speed and electromagnetic torque on full load at 150rad/sec speed.

6.3.2 FOC Scheme Results at Different Speeds

The stator current, rotor speed and electromagnetic torque of field oriented control scheme for different speeds is shown in the following figures. Figure 6.16 shows the full load torque results at a speed of 50rad/sec, figure 6.17 shows results at 100rad/sec, figure 6.18 shows results at 150rad/sec and figure 6.19 shows results at 200rad/sec.

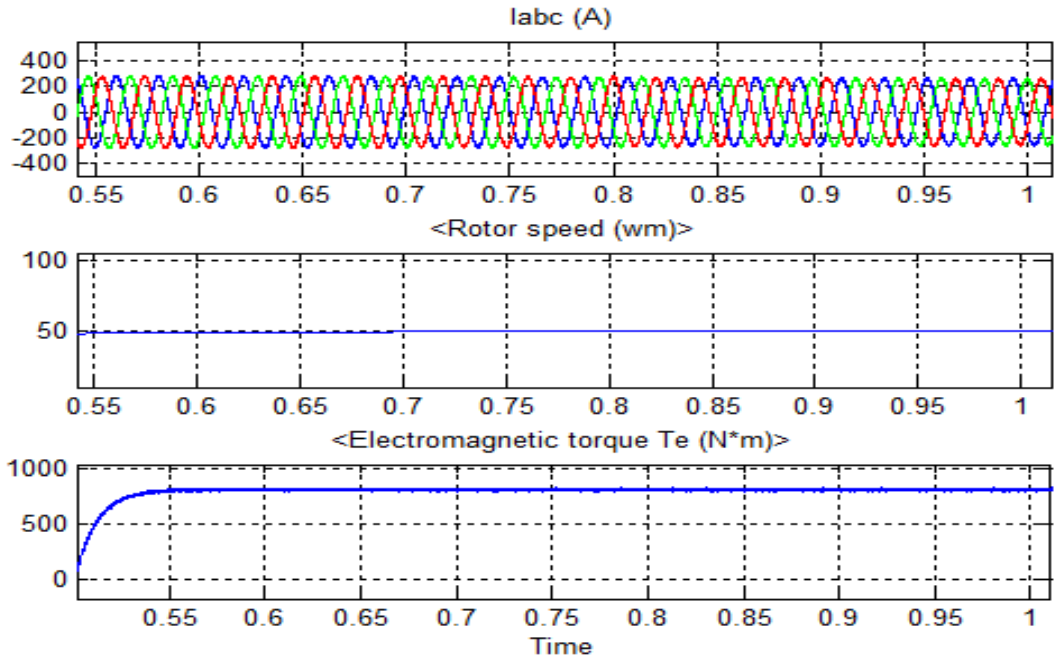

Figure 6.15 Simulink plot for FOC scheme showing three phase stator current, speed and electromagnetic torque for full load (800Nm) at 50rad/sec speed

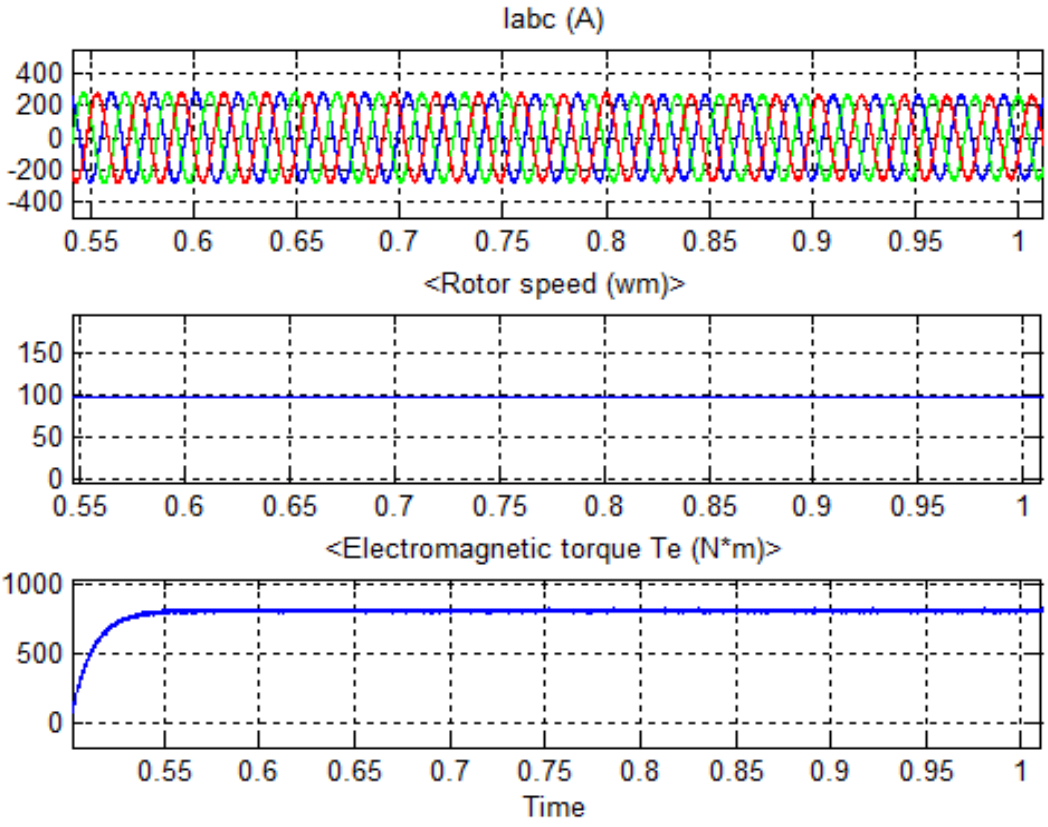

Figure 6.16 Simulink plot for FOC scheme showing three phase stator current, speed and electromagnetic torque for full load (800Nm) at 100rad/sec speed

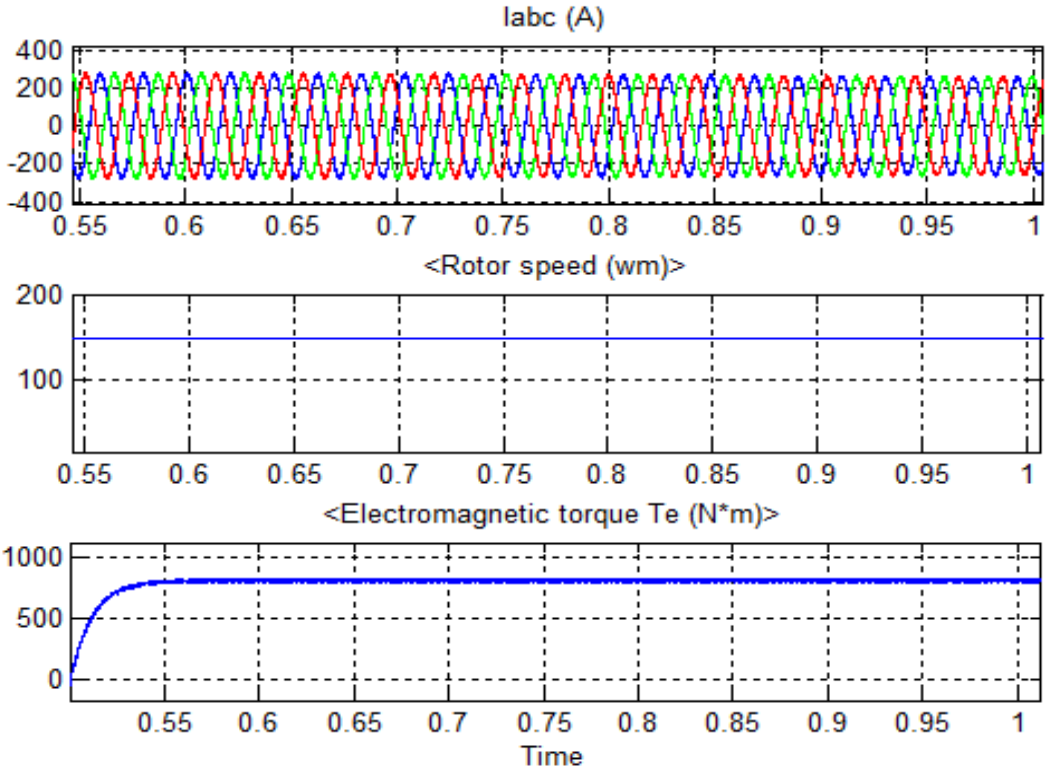

Figure 6.17 Simulink plot for FOC scheme showing three phase stator current, speed and electromagnetic torque for full load (800Nm) at 150rad/sec speed

6.4 DC Link Voltage Variations for Supply Perturbations

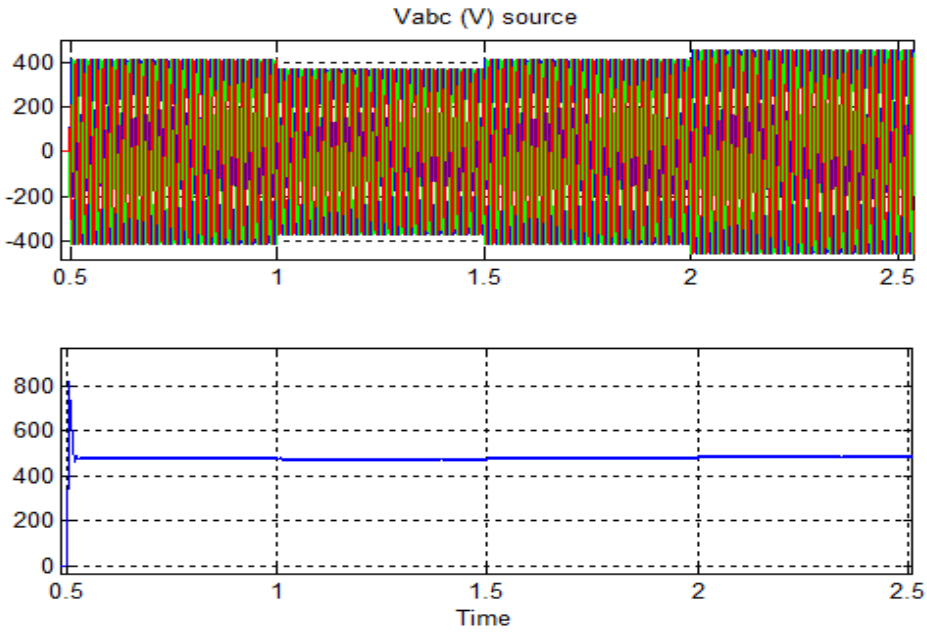

Figure 6.18 Simulink plot for DC link voltage with supply perturbations

Figure 6.18 shows the simulink waveform for the dc link voltage when supply voltage is perturbed for ±10%. In this simulation the normal supply voltage of 415V is supplied at 0.5s and is perturbed after every .5 seconds interval. The corresponding values of DC link voltage for step change of 10% in supply voltage at interval of 0.5 seconds are shown in table II.

Table II. DC LINK VOLTAGE VARIATIONS FOR SUPPLY VOLTAGE PERTURBATIONS .

Time (seconds)	Supply Voltage (V)	DC Link Voltage (V)
0.5	415	480
1	370	476
1.5	415	480
2	460	484

According to the observation of readings from table II, it is inferred that for supply voltage variation of 10%, change in DC link voltage is of 1% which is unobservable.

6.5 Comparison of FOC and DTC Scheme Results

The simulation results of DTC methods are shown in figure 6.1 to figure 6.9. The results for electromagnetic torque, rotor speed and stator currents at no load half load and full load condition for the reference speed at 150 rad/sec are shown in figure 6.4, figure 6.5 and figure 6.6respectively.

The simulation results of FOC methods are shown in figure 6.10 to figure 6.17. The results for electromagnetic torque, rotor speed and stator currents at no load half load and full load condition for the reference speed at 150 rad/sec are shown in figure 6.12, figure 6.13 and figure 6.14 respectively.

Table III shows the comparison between the time period required to attain steady state and steady state torque oscillations for FOC and DTC schemes with reference to their results shown in figure (6.4-6.6) and figure (6.12-6.14) for different percentage loading at a given speed of 150 rad/sec. In DTC scheme, time to attain steady state remain relatively constant at 0.53 seconds, whereas in case of FOC time to attain steady state is less for no load and remains same for half and full load.

Table III. COMPARISON OF CONTROL SCHEMES AT DIFFERENT LOADS

% Loading	**Type of Control Scheme**	**Time to attain steady state(s)**	**Steady state torque oscillations (%)**
No Load	FOC	0.5	±1.25
	DTC	0.53	±4.375
50% load	FOC	0.56	±1.875
	DTC	0.53	±4.375
Full Load	FOC	0.56	±1.875
	DTC	0.53	±4.375

It is observed that the torque oscillations in FOC control scheme are negligible whereas in DTC scheme oscillations in torque are observed. The oscillations for DTC scheme are rather constant and are more noticeable than FOC.

Table IV shows the comparison between the time required to attain steady state and steady state torque oscillations for FOC and DTC control schemes with reference to results shown in figure (6.7-6.9) and figure (6.15-6.17) for different speeds at full load (800 Nm). Different speeds taken are as follows: 50 rad/s, 100 rad/s, 150 rad/s. Table IV shows that time to attain steady state is constant for different speeds for both schemes.

Table IV. COMPARISON OF CONTROL SCHEMES AT DIFFERENT SPEEDS

Different Speeds	**Type of Control Scheme**	**Time to attain steady state(s)**	**Steady state torque oscillations (%)**
50 rad/sec	FOC	0.56	±1.875
	DTC	0.53	±5
100 rad/sec	FOC	0.56	±1.875
	DTC	0.53	±4.375
150 rad/sec	FOC	0.56	±1.875
	DTC	0.53	±4.375

Similarly, torque oscillations at low speed are comparatively higher, and then decreases with increase in speed for DTC control scheme however remains constant for FOC. The comparison as shown in table III and IV shows that DTC scheme attains faster steady state than FOC, whereas torque oscillations are smaller in case of FOC.

The PWM converter is designed for industrial drives and it can be seen from figure 6.3 and figure 6.11, the power factor on the source side is maintained at unity. The harmonics on the source side are also within IEEE 519 standards. The total harmonic distortion of DTC scheme for full load is 7.35% and for FOC scheme is 8.13%.

CHAPTER 7
CONCLUSIONS AND FURTHER SCOPE OF WORK

CHAPTER 7
CONCLUSIONS AND FURTHER SCOPE OF WORK

7.1 Conclusion

This thesis presents a comparison between two vector control methods for industrial induction motor drives: Field oriented control and direct torque control. The simulation studies are carried out for 200hp motor. Both methods provide a decoupled control of torque and flux during transients and steady-state.

Simulink model of induction motor drives has been presented, different Simulink block such as hysteresis current regulator, flux calculation block, theta calculation block, PI controller, unity power factor controller, abc to d-q and d-q to abc, current controller, PLL, PWM generator has been discussed and explained.

With DTC control scheme the motor attains steady state much faster but have oscillations in the torque whereas with FOC the oscillations in the torque are much smaller but takes more time to attain steady state. So, depending upon the needs of a particular application one method can be more suitable than the other.

The PWM Converter is designed to control the harmonic and power factor on the source side. The THD of the system is well within IEEE standards.

7.2 Future Scope of Work

There are several important points which needs to be investigated but could not be covered in this work due to the limited time frame. Some of these significant points need an immediate investigation for future works in order to take maximum advantage of this work. A number of intelligent controllers as fuzzy, neuro fuzzy are available today that can be implemented for control of industrial induction motor drive to further increase their performance and improve response time. The performance of PWM converter and drives controller with the proposed schemes is reported in this thesis, with its scope limited to simulation only. The work can be further extended for real time implementation.

The topologies proposed can also be integrated with the PLC and SCADA system for distributed control of many drives in industries and production plants.

It is hoped that the control scheme and topologies reported in this thesis will help in establishing new designs and control schemes for PWM converters and drives control strategies.

APPENDIX

Motor Parameters

The induction machine used in the MATLAB /simulation is 3phase, 1500rpm, 50Hz induction machine having the following parameters.

Power output	200HP
Rated Voltage	480V
R_s (stator resistance)	0.01485Ω
R_r (rotor resistance)	0.3295Ω
L_s (stator inductance)	0.0003027H
L_r (rotor inductance)	0.0003027H
L_m (magnetizing inductance)	0.01046H
J (moment of inertia)	3.1Kg m^2
P (number of poles)	4
Ns (Synchronous Speed)	157 rad/sec

REFERENCES

[1] F. Blaschke, " *The principle of field orientation as applied to new transvector closed loop control system for rotating field machine,*" Siemens Rev, vol. 34,,pp 217-220'May 1972.

[2] Mohan N., Undeland T., Robbins W. "*Power Electronics, Converters, Applications and Design*". Second Edition. John Wiley & Sons, Inc. USA. 1995. 802p. ISBN : 0-471-30576-6

[3] Depenbrock, "*Direct self control (DSC) of inverter-fed induction machines*" , IEEE Trans. Power Electronics, vol. 3, no. 4, pp. 420-429, 988.

[4] Muhammad H. Rashid. "*Power Electronic Handbook, Devices, Circuits, and Applications*". Second Edition. Burlington, MA : Academic. 2006. 1172p. ISBN: 978-0-12-088479-7.

[5] Blasko V., Kaura V. "*A New Mathematical Model and Control of a Three Phase AC–DC Voltage Source Converter*". IEEE Transactions on Power Electronics, 1997 Vol.12, issue: 1. Pages: 116 –123.

[6] Rupprecht Gabriel. Werner Leonhard, and Craig J. Nordby, "*Field-Oriented Control of a Standard AC Motor Using Microprocessors*", IEEE Transactions On Industrial Applications vol. ia-16, no. 2, march/april 1980

[7] K. Hasse, "*Zur dynamik drehzahlgeregelter antriebe mit stromrichtergespeisten asynchrony-kurzschlublaufenn- aschinen*", Darmstadt, Techn. Hochsch., Diss., 1969.

[8] Masato Koyama, Masao Yano, Isao Kamiyama, And Sadanari Yano, "*Microprocessor-Based Vector Control System For Induction Motor Drives With Rotor Time Constant Identification Function*", *IEEE Transactions on Industry Applications*, vol. ia-22, no. 3, may/june 1986

[9] Marian P. Kazmierkowski And Waldemar Sulkowski, "*A Novel Vector Control Scheme For Transistor PWM Inverter-Fed Induction Motor Drive", IEEE Transactions On Industrial Electronics*, vol. 38, no. 1, february 1991

[10] Takayoshi Matsuo and Thomas A. Lipo, "*A Rotor Parameter Identification Scheme forVector-Controlled Induction Motor Drives*", *IEEE Transactions On Industry Applications*, vol. ia-21, no. 4, may/june 1985.

[11] Hebertt Sira-Ramírez, Felipe González-Montañez, John Alexander Cortés-Romero and Alberto Luviano-Juárez, "*A Robust Linear Field-Oriented Voltage Control for the Induction Motor: Experimental Results*", IEEE Transactions On Industrial Electronics, Vol. 60, No. 8, 0278-0046, August 2013.

[12] Zhen and Longya Xu, "*On-Line Fuzzy Tuning of Indirect Field-Oriented an Induction Machine Drives"*, IEEE Transactions on Power Electronics, Vol. 13, No. 1, pp. 134-138, January 1998.

[13] Bimal.K. Bose, Nitin R Patel, and Kaushik Rahashekara, "*A Neuro Fuzzy Based On-Line Efficiency Optimization Control of a Stator Flux-Oriented Direct Vector-Controlled Induction Motor Drive*" IEEE Trans. Industrial Electronics, Vol.4 0278-0046/97-01822-4, April, 1997.

[14] N. Mariun, S. B Mohd Noor, J. Jasni, and O. S. Bennanes, "*A Fuzzy Logic Based Controller For An Indirect Vector Controlled Three-Phase Induction Motor*" IEEE IECON Conf. Rec., Vol. 4, pp. 1-4, Nov. 2004.

[15] J.W Finch, DJ Atkinson and PP Acarnleg University of Newcastle up on Tyne, UK, "*General Principles of Modern Induction motor control*"

[16] Vas, P. "*Sensor less Vector and Direct Torque Control*". Oxford University Press 1998.

[17] I. Takashi and T. Noguchi, "*A new quick-response and high-efficiency control of an induction motor*", IEEE Trans. Industry Applications, vol. A-22, no.5, pp. 820-827, 1986.

[18] Schauder, C, " *Adaptive speed identification for vector control of induction motors without rotational transducers.*" IEEE Trans. Industrial Applications, vol.28, pp. 1054-1061, 1992

[19] D.Casadei, G.Serra, and A.Tani, "*Implementation of a direct torque control algorithm for induction motors based on discrete space vector modulation*" IEEE Trans. Power Electron., vol. 15, pp. 769-777, July, 2000.

[20] L. Tang, M.F. Rahman, "*A new direct torque control strategy for flux and torque ripple reduction for induction motors drive by using space vector modulation*" IEEE 32nd Annual Power Electronics Specialists conference, PESC 2001, vol. 3, pp. 1440-1445, 2001.

[21] A. Kumar, B.G. Fernandes, and K. Chatterjee, "*Simplified SVPWMDTC f 3-phase induction motor using the concept of imaginary witching times*" The 30th Annual Conference of the IEEE Industrial Electronics Society, Korea, pp. 341-346, 2004.

[22] H.R. Keyhani, M.R. Zolghadri, and A. Homaifar, "*An extended and improved discrete space vector modulation direct torque control for induction motors*", 35th Annual IEEE Power Electronics Specialists conference, Germany, pp. 3414-3420, 2004.

[23] C. Martins, X. Roboam, T.A. Meynard, and A.S. Caryolha, " *Switching frequency imposition and ripple reduction in DTC drives by using a multilevel converter,* " IEEE Trans. Power Electron., vol. 17, pp.286-297, Mar. 2002

[24] Zhe Zhang, Student Member, IEEE, Yue Zhao, Student Member, IEEE, Wei Qiao, Senior Member, IEEE, and Liyan Qu, Member, IEEE, "*A Space-Vector Modulated Sensorless Direct-Torque Control for Direct-Drive PMSG Wind Turbines*", IEEE Transactions on Industry Applications, 2013-IACC-468, 0093-9994, Decmber-2013.

[25] Johnny Rengifo, José Aller, Alberto Berzoy and José Restre, "*Predictive DTC algorithm for Induction Machines using Sliding Horizon Prediction*", IEEE, 978-1-4799-2507-0/14, 2014.

[26] A. SchÄonung and H. Stemmler, "*Static frequency changer with sub harmonics control in conjunction with reversible variable speed AC drives,*" Brown Boweri Rev. 51, pp. 555 { 577}, 1964.

[27] Juan W. Dixan and Boon T. Ooi, "*Series and Parallel Operation of Hysteresis Current-Controlled PWM Rectifiers*", IEEE Transactions on Industrial Applications, vol. 25, no. 4, pp. 644.651, July/August 1989.

[28] S.B. Dewan, R.Wu, "*A PWM ac to dc converter with fixed switching frequency,*" in conf. Rec. 1987 IEEE-IAS Ann. Meeting, pp. 706-711

[29] Bo Yin, Oruganti R., Panda S.K., Bhat A.K.S. "*A Simple Single Input Single Output (SISO) Model for a Three Phase PWM Rectifier*". IEEE Transactions on Power Electronics, 2009. Vol.24, issue: 3. Pages: 620 – 631.

[30] Hengchun Mao, Boroyevich D., Lee F.C.Y. "*Novel Reduced Order Small Signal Model of a Three Phase PWM Rectifier and Its Application in Control*

Design and System Analysis". IEEE Transactions on Power Electronics, 1998. Vol.13, issue: 3. Pages: 511 – 521.

[31] Hiti S., Boroyevich D., Cuadros, C. "*Small signal modeling and control of three phase PWM converters*". Industry Applications Society Annual Meeting, IEEE 1994. Vol.2, pages: 1143 – 1150.

[32] H.S. KIM, H.S. MOK, G.H. CHOE, D.S. HYUN, S.Y. CHOE. "*Design of Current Controller for 3 Phase PWM Converter with Unbalanced Input Voltage*". Power Electronics Specialists Conference, IEEE 1998. Vol.1. Pages: 503 – 509.

[33] Hava Ahmet M., Kerkman Russel J., Lipo Thomas A. "*Carrier Based PWM VSI Overmodulation Strategies : Analysis, Comparison, and Design*". IEEE Transactions on Power Electronics, 1998, Vol.13, issue: 4, pages: 674 – 689.

[34] Amuda L.N., Cardoso Filho B.J., Silva S.M., Silva S.R., Diniz A.S.A.C. "*Wide bandwidth single and three phase PLL structures for grid tied PV systems*". Photovoltaic Specialists Conference, IEEE 2000. Pages: 1660 – 1663.

[35] Salamah A.M. "*Three phase phase lock loop for distorted utilities*". IET Electric Power Applications, 2007. Vol.1, issue : 6, pages: 937–945.

LIST OF PUBLICATIONS

- Garg Rachana, Mahajan Priya, Gupta Nikita and Saroa Harsha *A Comparative Study between Field Oriented Control and Direct Torque Control of AC Traction Motor* IEEE International Conference on recent advances and innovation in engineering(icraie-2014) May 09-11, 2014, Jaipur India
- Garg Rachana, Saroa Harsha and Gupta Nikita *Design and Development of Prototype Distribution System* National conference on IPRoMM-2014.
- Garg Rachana, Gupta Nikita and Saroa Harsha *Symmetrical and Non-Symmetrical Fault Simulation by DIgSILENT Power Factory Software* National conference on IPRoMM-2014
- Saroa Harsha and Gupta Nikita *Hardware Implementation of Prototype Model Of Two Port Network* International Conference of Advance Research and Innovation
- Dogra Rahul, Gupta Nikita and Saroa Harsha *Economic Load Dispatch Problem and MATLAB Programming Of Different Methods.* International Conference of Advance Research and Innovation.